



Teanby, N. A., Showman, A., Flecher, L., & Irwin, P. G. J. (2014). Constraints on Jupiter's Stratospheric HCl abundance and chlorine cycle from Herschel/HIFI. *Planetary and Space Science*, 103, 250-261. 10.1016/j.pss.2014.07.015

Link to published version (if available):
[10.1016/j.pss.2014.07.015](https://doi.org/10.1016/j.pss.2014.07.015)

[Link to publication record in Explore Bristol Research](#)
PDF-document

University of Bristol - Explore Bristol Research

General rights

This document is made available in accordance with publisher policies. Please cite only the published version using the reference above. Full terms of use are available:
<http://www.bristol.ac.uk/pure/about/ebr-terms.html>

Take down policy

Explore Bristol Research is a digital archive and the intention is that deposited content should not be removed. However, if you believe that this version of the work breaches copyright law please contact open-access@bristol.ac.uk and include the following information in your message:

- Your contact details
- Bibliographic details for the item, including a URL
- An outline of the nature of the complaint

On receipt of your message the Open Access Team will immediately investigate your claim, make an initial judgement of the validity of the claim and, where appropriate, withdraw the item in question from public view.

Manuscript Number:

Title: Constraints on Jupiter's Stratospheric HCl abundance and chlorine cycle from Herschel/HIFI

Article Type: Research Paper

Keywords: Jupiter; Atmosphere; Composition; Photochemistry; Herschel; sub-millimetre

Corresponding Author: Dr. Nicholas A. Teanby, Ph.D.

Corresponding Author's Institution: University of Bristol

First Author: Nicholas A. Teanby, Ph.D.

Order of Authors: Nicholas A. Teanby, Ph.D.; Adam P Showman, Ph.D.; Leigh N Fletcher, Ph.D.; Patrick G Irwin, Ph.D.

Abstract: Detection of HCl on Jupiter would provide insight into the chlorine cycle and external elemental fluxes on giant planets, yet so far has not been possible. Here we present the most sensitive search for Jupiter's stratospheric HCl to date using observations of the 625.907 and 1876.221 GHz spectral lines with Herschel's HIFI instrument. HCl was not detected, but we determined the most stringent upper limits so far, improving on previous studies by two orders of magnitude. If HCl is assumed to be uniformly mixed, with a constant volume mixing ratio above the 1 mbar pressure level and has zero abundance below, we obtain a 3-sigma upper limit of 0.056 ppb; in contrast, if we assume uniform mixing above the 1~mbar level and allow a non-zero but downward-decreasing abundance from 1~mbar to the troposphere based on eddy diffusion, we obtain a 3-sigma upper limit of 0.024 ppb. This is below the abundance expected for a solar composition source, such as comets, and implies that upper atmosphere HCl loss processes are important. We investigated aerosol scavenging using a simple diffusion model and conclude that it could be a very effective mechanism for HCl removal. Transient scavenging by stratospheric NH₃ from impacts is another potentially important loss mechanism. This suggests that it is extremely unlikely that HCl is present in sufficient quantities to be detectable in the near future. We summarise the implications for Jupiter's chlorine cycle and conclude that based on a combination of our observations and previous studies of external oxygen supply, a solar composition external source for Jupiter's chlorine combined with stratospheric scavenging by aerosols and NH₃ appears the most plausible.

Highlights (for review)

HIFI/Herschel observations were used to determine upper limits for HCl on Jupiter

3-sigma upper limits are 0.056 ppb (uniform profile) and 0.024 ppb (varying profile)

Scavenging by stratospheric aerosols could explain the low upper limits

Results are most consistent with a cometary source for Jupiter's chlorine

Constraints on Jupiter's Stratospheric HCl abundance and chlorine cycle from Herschel/HIFI[☆]

N. A. Teanby^a, A. P. Showman^b, L. N. Fletcher^c, P. G. J. Irwin^c

^a*School of Earth Sciences, University of Bristol, Wills Memorial Building, Queen's Road, Bristol, BS8 1RJ, U.K.*

^b*Lunar & Planetary Laboratory, University of Arizona, Tucson, Arizona, USA.*

^c*Atmospheric, Oceanic & Planetary Physics, Department of Physics, University of Oxford, Clarendon Laboratory, Parks Road, Oxford, OX1 3PU. UK.*

Abstract

Detection of HCl on Jupiter would provide insight into the chlorine cycle and external elemental fluxes on giant planets, yet so far has not been possible. Here we present the most sensitive search for Jupiter's stratospheric HCl to date using observations of the 625.907 and 1876.221 GHz spectral lines with Herschel's HIFI instrument. HCl was not detected, but we determined the most stringent upper limits so far, improving on previous studies by two orders of magnitude. If HCl is assumed to be uniformly mixed, with a constant volume mixing ratio above the 1 mbar pressure level and has zero abundance below, we obtain a 3- σ upper limit of 0.056 ppb; in contrast, if we assume uniform mixing above the 1 mbar level and allow a non-zero but downward-decreasing abundance from 1 mbar to the troposphere based on eddy diffusion, we obtain a 3- σ upper limit of 0.024 ppb. This is below the abundance expected for a solar composition source, such as comets, and

[☆]*Herschel* is an ESA space observatory with science instruments provided by European-led Principal Investigator consortia and with important participation from NASA.

Email address: n.teanby@bristol.ac.uk (N. A. Teanby)

1
2
3
4
5
6
7
8
9 implies that upper atmosphere HCl loss processes are important. We inves-
10 tigated aerosol scavenging using a simple diffusion model and conclude that
11 it could be a very effective mechanism for HCl removal. Transient scaveng-
12 ing by stratospheric NH₃ from impacts is another potentially important loss
13 mechanism. This suggests that it is extremely unlikely that HCl is present in
14 sufficient quantities to be detectable in the near future. We summarise the
15 implications for Jupiter’s chlorine cycle and conclude that based on a combi-
16 nation of our observations and previous studies of external oxygen supply, a
17 solar composition external source for Jupiter’s chlorine combined with strato-
18 spheric scavenging by aerosols and NH₃ appears the most plausible.
19

20
21
22
23
24
25
26
27
28 *Keywords:* Jupiter, Atmosphere, Composition, Photochemistry, Herschel,
29 sub-millimetre
30

31
32
33 **1. Introduction**
34

35
36
37
38
39
40
41
42
43
44
45
46
47
48
49
50
51
52
53
54
55
56
57
58
59
60
61
62
63
64
65
66
67
68
69
70
71
72
73
74
75
76
77
78
79
80
81
82
83
84
85
86
87
88
89
90
91
92
93
94
95
96
97
98
99
100
101
102
103
104
105
106
107
108
109
110
111
112
113
114
115
116
117
118
119
120
121
122
123
124
125
126
127
128
129
130
131
132
133
134
135
136
137
138
139
140
141
142
143
144
145
146
147
148
149
150
151
152
153
154
155
156
157
158
159
160
161
162
163
164
165
166
167
168
169
170
171
172
173
174
175
176
177
178
179
180
181
182
183
184
185
186
187
188
189
190
191
192
193
194
195
196
197
198
199
200
201
202
203
204
205
206
207
208
209
210
211
212
213
214
215
216
217
218
219
220
221
222
223
224
225
226
227
228
229
230
231
232
233
234
235
236
237
238
239
240
241
242
243
244
245
246
247
248
249
250
251
252
253
254
255
256
257
258
259
260
261
262
263
264
265
266
267
268
269
270
271
272
273
274
275
276
277
278
279
280
281
282
283
284
285
286
287
288
289
290
291
292
293
294
295
296
297
298
299
300
301
302
303
304
305
306
307
308
309
310
311
312
313
314
315
316
317
318
319
320
321
322
323
324
325
326
327
328
329
330
331
332
333
334
335
336
337
338
339
340
341
342
343
344
345
346
347
348
349
350
351
352
353
354
355
356
357
358
359
360
361
362
363
364
365
366
367
368
369
370
371
372
373
374
375
376
377
378
379
380
381
382
383
384
385
386
387
388
389
390
391
392
393
394
395
396
397
398
399
400
401
402
403
404
405
406
407
408
409
410
411
412
413
414
415
416
417
418
419
420
421
422
423
424
425
426
427
428
429
430
431
432
433
434
435
436
437
438
439
440
441
442
443
444
445
446
447
448
449
450
451
452
453
454
455
456
457
458
459
460
461
462
463
464
465
466
467
468
469
470
471
472
473
474
475
476
477
478
479
480
481
482
483
484
485
486
487
488
489
490
491
492
493
494
495
496
497
498
499
500
501
502
503
504
505
506
507
508
509
510
511
512
513
514
515
516
517
518
519
520
521
522
523
524
525
526
527
528
529
530
531
532
533
534
535
536
537
538
539
540
541
542
543
544
545
546
547
548
549
550
551
552
553
554
555
556
557
558
559
560
561
562
563
564
565
566
567
568
569
570
571
572
573
574
575
576
577
578
579
580
581
582
583
584
585
586
587
588
589
590
591
592
593
594
595
596
597
598
599
600
601
602
603
604
605
606
607
608
609
610
611
612
613
614
615
616
617
618
619
620
621
622
623
624
625
626
627
628
629
630
631
632
633
634
635
636
637
638
639
640
641
642
643
644
645
646
647
648
649
650
651
652
653
654
655
656
657
658
659
660
661
662
663
664
665
666
667
668
669
670
671
672
673
674
675
676
677
678
679
680
681
682
683
684
685
686
687
688
689
690
691
692
693
694
695
696
697
698
699
700
701
702
703
704
705
706
707
708
709
710
711
712
713
714
715
716
717
718
719
720
721
722
723
724
725
726
727
728
729
730
731
732
733
734
735
736
737
738
739
740
741
742
743
744
745
746
747
748
749
750
751
752
753
754
755
756
757
758
759
760
761
762
763
764
765
766
767
768
769
770
771
772
773
774
775
776
777
778
779
780
781
782
783
784
785
786
787
788
789
790
791
792
793
794
795
796
797
798
799
800
801
802
803
804
805
806
807
808
809
810
811
812
813
814
815
816
817
818
819
820
821
822
823
824
825
826
827
828
829
830
831
832
833
834
835
836
837
838
839
840
841
842
843
844
845
846
847
848
849
850
851
852
853
854
855
856
857
858
859
860
861
862
863
864
865
866
867
868
869
870
871
872
873
874
875
876
877
878
879
880
881
882
883
884
885
886
887
888
889
890
891
892
893
894
895
896
897
898
899
900
901
902
903
904
905
906
907
908
909
910
911
912
913
914
915
916
917
918
919
920
921
922
923
924
925
926
927
928
929
930
931
932
933
934
935
936
937
938
939
940
941
942
943
944
945
946
947
948
949
950
951
952
953
954
955
956
957
958
959
960
961
962
963
964
965
966
967
968
969
970
971
972
973
974
975
976
977
978
979
980
981
982
983
984
985
986
987
988
989
990
991
992
993
994
995
996
997
998
999
1000

Detection of HCl provides the potential to reveal unique aspects of chem-
ical, dynamical, and external supply processes on the giant planets. HCl
abundance is expected to be extremely variable throughout the atmospheric
column and will depend strongly on local atmospheric conditions and the
nature of the source reservoir. At the most basic level, Jupiter’s bulk chlo-
rine abundance can be estimated from the solar chlorine to hydrogen ratio of
 3.2×10^{-6} (Grevesse et al., 2007) combined with the observation that Jupiter
is enriched in heavy elements, such as carbon, relative to the solar compo-
sition by a factor of about four (Niemann et al., 1998; Wong et al., 2004).
If all chlorine is present as HCl and no other processes were occurring, we
would expect relative abundances of order 10 ppm based on this argument.

1
2
3
4
5
6
7
8
9
10 13 Such high amounts are not present in the observable upper atmosphere and
11 14 more advanced treatment is required.

12
13 15 Comprehensive thermochemical models of Jupiter's deep interior predict
14 16 that chlorine is predominantly in the form of HCl (Fegley and Lodders, 1994).
15 16 However, at pressures less than about 20 bar the temperature drops below
16 17 400K and HCl is removed by reaction with tropospheric ammonia (NH_3) to
17 18 form ammonia salts (NH_4Cl). This reaction is predicted to be extremely
18 19 fast, so that any HCl dredged up from the deep interior by convection would
19 20 be immediately removed before it could reach observable atmospheric levels
20 21 (Fegley and Lodders, 1994; Showman, 2001). Therefore, we do not expect
21 22 to see any signature from Jupiter's deep HCl reservoir in the stratosphere or
22 23 upper troposphere.
23 24

24 25 Another potential source for HCl is externally from comets, interplane-
25 26 tary dust particles, meteoroids, rings particles, or satellites - especially the
26 27 volcanic moon Io. Observations of trace stratospheric species show the sup-
27 28 ply of external material to Jupiter's atmosphere is significant (Feuchtgruber
28 29 et al., 1999; Bézard et al., 2002; Lellouch et al., 2002; Fletcher et al., 2011)
29 30 and forms an important but poorly understood part of the upper atmosphere
30 31 chemistry. HCl from external sources would be deposited directly into the
31 32 stratosphere. Importantly, troposphericly sourced ammonia will have been
32 33 effectively entirely removed before it reaches the upper stratosphere by a
33 34 combination of condensation at the tropopause cold trap and photodissoci-
34 35 ation reactions (Atreya et al., 1977; Atreya and Donahue, 1979). Therefore,
35 36 externally sourced HCl could avoid removal by reactions with tropospheric
36 37 ammonia and potentially persist in observable quantities in the upper strato-
37

1
2
3
4
5
6
7
8
9 sphere and mesosphere (Showman, 2001).

10 HCl has extremely strong rotational spectral transitions in the far-IR
11 and sub-mm, which when combined with the expectation of potentially sig-
12 nificant stratospheric abundances derived from external sources, make it a
13 promising target for spectroscopic detection. Measurements of the amount
14 of HCl in Jupiter's stratosphere would provide constraints on the chlorine
15 cycle and external flux sources and magnitudes. However, despite a long
16 campaign of observations, detection of any halide compound (HCl, HF, HBr,
17 or HI) on any giant planet has remained elusive (Noll, 1996; Weisstein and
18 Serabyn, 1996; Kerola et al., 1997; Fouchet et al., 2004; Teanby et al., 2006;
19 Fletcher et al., 2012). The closest to a positive detection on any of the giant
20 planets was by Weisstein and Serabyn (1996) who produced a tentative de-
21 tection of 1.1 ppb (parts per billion) HCl on Saturn. However, this was not
22 confirmed by subsequent more sensitive space-based studies, which obtained
23 upper limits of 6.7×10^{-11} (Teanby et al., 2006) and 3.8×10^{-11} (Fletcher et al.,
24 2012) appropriate for the 0.5 bar pressure level. This highlights some of the
25 difficulties of observing halide compounds. The strongest HCl lines occur at
26 frequencies higher than 1 THz, which are not measurable using ground-based
27 telescopes, so weaker lower frequency lines must be used that are susceptible
28 to contamination by telluric water vapour, resulting in much lower sensitiv-
29 ities. Conversely, observations from space-based orbiters tend to have lower
30 spectral resolution and reduced sensitivities to narrow spectral lines.

31
32
33
34
35
36
37
38
39
40
41
42
43
44
45
46
47
48
49
50
51 In the absence of any previous detections of HCl, the external flux of ma-
52 terial into Jupiter's atmosphere can be estimated from the observed strato-
53 spheric abundances of oxygen species (Feuchtgruber et al., 1997; Feuchtgru-
54
55
56
57
58
59
60
61
62
63
64
65

1
2
3
4
5
6
7
8
9
10 ber et al., 1999; Bézard et al., 2002), which imply an oxygen flux of $1\text{--}4\times 10^6$
11 atoms/cm²/s. Assuming a solar relative elemental abundance for Cl/O of
12
13 6.9×10^{-4} (Grevesse et al., 2007) implies a very low external meteoric chlo-
14
15 rine (Cl) flux of around 700–2800 atoms/cm²/s.
16

17 However, if instead the dominant contribution to Jupiter’s external Cl
18
19 flux is from Io’s plasma torus, which contains a significant amount of chlo-
20
21 rine (Küppers and Schneider, 2000). Showman (2001) estimates that the
22
23 total chlorine flux could be much higher: 3×10^6 atoms/cm²/s if all of Io’s
24
25 torus material eventually enters Jupiter’s atmosphere; or a more reasonable
26
27 7×10^4 atoms/cm²/s for an entry fraction based on the measured Cl/O ratios
28
29 and external oxygen flux. Showman (2001) used the latter Cl flux with a
30
31 1D diffusion-transport model to predict a maximum abundance of HCl in
32
33 Jupiter’s stratosphere. At the 1 mbar pressure level the model predicted
34
35 1 ppb HCl in Jupiter’s upper stratosphere, with a sharp decrease in abun-
36
37 dance with increasing pressures caused by vertical mixing. The modelled
38
39 profile is most appropriate for the stratosphere as there is expected to be sig-
40
41 nificant scavenging from ammonia in the troposphere which was not included
42
43 in the diffusion profile calculation. However, for the purpose of comparison
44
45 with previously published upper limits, the model can be used to predict an
46
47 upper bound on externally sourced HCl at around 0.5 bar of $\sim 3\times 10^{-13}$ for
48
49 Jupiter and $\sim 10^{-13}$ for Saturn. The model predictions are consistent with
50
51 the most stringent current upper limits for HCl in Jupiter’s troposphere of
52
53 2.3 ppb derived by Fouchet et al. (2004) using Cassini’s CIRS instrument
54
55 (Flasar et al., 2004). The predictions are also consistent with upper limits de-
56
57 rived for Saturn of 6.7×10^{-11} determined by Teanby et al. (2006) using CIRS
58
59
60
61
62
63
64
65

1
2
3
4
5
6
7
8
9
10 88 and 3.8×10^{-11} determined by Fletcher et al. (2012) using Herschel/SPIRE.
11 89 Therefore, further constraints on the vertical distribution require orders of
12
13 90 magnitude more sensitivity than previous measurements.

14
15 91 The Herschel space telescope was specifically designed to observe the sub-
16
17 92 mm spectral region and is ideally suited to a search for HCl, which should be
18
19 93 easily detectible on Jupiter if it is present in \sim ppb quantities at 1 mbar. Her-
20
21 94 schel's Heterodyne Instrument for the Far-Infrared (HIFI) (de Graauw et al.,
22
23 95 2010) provides the best opportunity to accurately measure Jupiter's strato-
24
25 96 spheric HCl for the foreseeable future, which motivates the present study;
26
27 97 there are no spacecraft with suitable remote sensing instruments scheduled
28
29 98 to visit Jupiter, or any other giant planet, for the next two decades at least.
30
31 99 HIFI's low noise and high spectral resolution means that our observations will
32
33 100 be sensitive to parts per trillion HCl levels - an improvement of around two
34
35 101 orders of magnitude on the best measurements currently available (Fouchet
36
37 102 et al., 2004). This allows us to place new constraints on Jupiter's chlorine
38
39 103 cycle.

40 41 104 **2. Observations**

42
43
44 105 Our HIFI observations were proposed as part of Herschel's OT1 call in
45
46 106 2010 (program ID: OT1_nteanby_2) and were observed on 28th February
47
48 107 and 7th March 2013 (just under two months before the coolant ran out
49
50 108 on 29th April 2013). We focused on the two HCl rotational bands that
51
52 109 had the maximum predicted signal-to-noise: 625.907 GHz in band 1; and
53
54 110 1876.221 GHz in band 7. Predicted signals were 0.082K at 625.907 GHz and
55
56 111 2.1K at 1876.221 GHz assuming an effective spectral resolution of 10 MHz

1
2
3
4
5
6
7
8
9
10 and an abundance profile with 1 ppb HCl for pressures less than 1 mbar.
11 We determined integration times using Herschel’s HSpot observation tool by
12
13 aiming for a high overall signal-to-noise ratio (S/N) of ~ 100 to allow for the
14
15 large uncertainties in HCl abundance. For band 1, total integration time
16
17 was 13600 seconds, split over three separate observations with a predicted
18
19 overall instrument noise level of 0.0012K per 10.5 MHz bandwidth and a S/N
20
21 of 70. For band 7, total integration time was 8742 seconds, again split over
22
23 three separate observations with a predicted overall instrument noise level of
24
25 0.016K per 10.5 MHz bandwidth and a S/N of 130.

26 Observations were taken in HIFI’s dual beam switch single point obser-
27
28 vation mode (HIFI Observers’ Manual, 2011), which resulted in maximum
29
30 efficiency within time allocation constraints. Both wide band spectrometer
31
32 (WBS) and high resolution spectrometer (HRS) were used, with resolutions
33
34 of 1.1 MHz and 0.25 MHz respectively. The WBS and HRS had the same
35
36 sensitivity for a given frequency interval, so the HRS data was only recorded
37
38 to provide information on the vertical profile of HCl in the case of a detec-
39
40 tion. As HCl was not detected we only consider the WBS measurements
41
42 here. Local oscillator frequencies of 620.303 GHz and 1873.233 GHz were
43
44 used and both upper and lower sidebands were measured. However, only the
45
46 upper side band is considered here as that contains the HCl lines; as expected
47
48 no other spectral features were observed in either side band. Horizontal and
49
50 vertical polarisations were measured separately. The WBS had a band width
51
52 of 4 GHz in band 1 and 2.4 GHz in band 7.

53 Observations had a single on-planet pointing centred on Jupiter, which
54
55 had an angular diameter of approximately $39''$. Herschel’s 3.28 m primary
56
57
58
59
60
61
62
63
64
65

1
2
3
4
5
6
7
8
9
10 137 mirror had Airy disc sizes of 36.7" and 12.3" in bands 1 and 7 respectively,
11 138 which resulted in disc-averaged spectra for band 1 and a low spatial resolution
12
13 139 disc-centred average for band 7; the effect of this on the observed spectra is
14
15 140 considered further in section 3.2. Full observation details are summarised in
16
17 141 Table 1.

142 **3. Data reduction**

143 *3.1. Level 2 data products*

144 Data were first processed using v10 of the standard HIPE pipeline (Ott,
145 2010) to give calibrated antenna temperatures T_a in both upper and lower
146 sidebands for each observation. Figure 1 shows the Level 2 post-pipeline
147 calibrated data, from which it is immediately obvious that the spectra were
148 affected by instrumental standing waves and long-period continuum ripples
149 with amplitudes of up to 4 K; much higher than the intrinsic instrument noise.
150 These standing waves are due to reflections within the instrument, which
151 result in quasi-sinusoidal interference with approximate periods of 92, 98,
152 100, and 320 MHz in bands 1 and 7 (Roelfsema et al., 2012). band 1 is most
153 affected by the 100 MHz standing waves, whereas band 7 is most affected
154 by the 320 MHz standing waves. Therefore, more advanced processing was
155 required before any useful information on HCl could be obtained.

156 *3.2. HCl lineshape*

157 Before performing any additional processing on the data, we first consider
158 the predicted signal in more detail and determine the exact shape of the HCl
159 emission lines, as this determines the level of standing wave removal that can

1
2
3
4
5
6
7
8
9
10 be achieved. If HCl can be assumed to exist above 1 mbar only, then the re-
11 sulting emission lines should be very narrow, with widths of <10 MHz. Such
12 narrow lines could be easily separated from the 100 MHz standing waves.
13 However, because of the large field-of-view and rapid rotation of Jupiter, the
14 major contribution to the effective observed line width is rotationally induced
15 doppler broadening. To calculate the line profile due to doppler broadening
16 we generated a synthetic image of Jupiter with 2001×2001 pixels, and for
17 each pixel calculated the emission angle, line-of-sight velocity, and associated
18 doppler shift. Each pixel was then weighted using Herschel's Airy disc and
19 the overall effective lineshape constructed from the weighted average con-
20 tribution from each pixel to the disc-averaged spectrum. A weighted mean
21 emission angle for each band was also calculated from the pixel map for use
22 in the radiative transfer modelling in section 4. Figure 2 shows the calculated
23 lineshapes for bands 1 and 7, which have full-width half maximum (FWHM)
24 of 35.39 MHz and 39.65 MHz respectively.
25
26
27
28
29
30
31
32
33
34
35
36
37
38

175 *3.3. Minimisation of standing wave interference*

176 By an unfortunate coincidence, Jupiter's rotation rate is such that the
177 FWHMs of the effective lineshapes are comparable to the FWHMs of the
178 92, 98, and 100 MHz instrumental standing waves (30.6, 32.7, and 33.3 MHz
179 respectively). This means that the standard HIPE baseline remove methods
180 could not be used without compromising the signal. Therefore, we developed
181 our own post-processing algorithm, taking great care not to adversely affect
182 any potential HCl signature. First, for each band, the six individual spec-
183 tra (3 x 2 polarisations) were high-pass filtered using a 4 pole Butterworth
184 filter (Gubbins, 2004) with a corner period of 200 MHz. This effectively

185 suppressed the 320 MHz standing waves and any long period continuum off-
 186 sets, resulting in spectra of antenna temperature difference ΔT_a relative to
 187 the baseline/continuum level. Second, for each band, the six spectra were
 188 binned and averaged with a bin width of 9 MHz to reduce the random noise.
 189 Any emission lines present would be much wider than these bins and would
 190 not be affected. Antenna temperature errors in each bin were calculated
 191 from the unweighted standard error of the six individual spectra. Third, a
 192 masked spectrum was produced by removing datapoints within ± 30 MHz of
 193 the HCl spectral lines in band 1 and ± 40 MHz of the the HCl spectral lines
 194 in band 7. This left spectra that were assumed to be composed entirely of
 195 standing waves and random noise (there are no other known gas lines in this
 196 range). Fourth, a least squares minimisation method was used to fit a single
 197 period sine wave to each of the masked spectra. The standing waves were
 198 not well represented by a single sine wave over the entire bandwidth, due to
 199 their quasi-sinusoidal nature, so the range fitted was limited to 2.2 GHz in
 200 band 1 and 1.5 GHz in band 7, which gave good fits around the predicted po-
 201 sitions of the HCl features. The fitted sine waves were assumed to represent
 202 the standing wave component and were removed from the binned spectra.
 203 These final processed spectra were converted from an antenna temperature
 204 difference ΔT_a into a main beam temperature difference ΔT_{mb} using:

$$\Delta T_{mb} = \Delta T_a \frac{\nu_l}{\nu_{mb}} \quad (1)$$

205 where ν_l is the forward efficiency and ν_{mb} is the main beam efficiency (Wilson
 206 et al., 2009; HIFI Observers' Manual, 2011). Instrument calibration gives
 207 $\nu_l = 0.96$, $\nu_{mb} = 0.76$ in band 1, and $\nu_{mb} = 0.69$ in band 7 (Roelfsema et al.,
 208 2012). To determine the brightness temperature difference ΔT_b , ΔT_{mb} was

1
2
3
4
5
6
7
8
9
209 divided by a fill factor s , which is the response weighted area of Jupiter that
10 intersects the main beam divided by the response weighted area of the main
11 beam. The values of s were 0.75 for band 1 and 1.00 for band 7. These
12
13
211 beam. The values of s were 0.75 for band 1 and 1.00 for band 7. These
14
15
212 data processing stages are illustrated in Figure 3. The final noise levels
16
17
213 were about 0.05–0.1K in both bands. While this method gives an order
18
19
214 of magnitude improvement in the noise over the standard pipeline product,
20
21
215 the noise levels are still higher than those predicted using HSpot by a factor
22
23
216 of 40–80 for band 1 and 3–6 for band 7. Band 1 is severely affected by
24
25
217 ~ 100 MHz standing waves, whereas the 320 MHz standing waves which are
26
27
218 more prevalent in band 7 are more easily removed. The HCl emission lines
28
29
219 are also much stronger in band 7, meaning that band 7 provides by far the
30
31
220 most powerful constraint on Jupiter’s HCl.

221 **4. Spectral modelling**

222 The change in brightness temperature due to HCl was calculated using the
223 NEMESIS radiative transfer code (Irwin et al., 2008). This has been used
224 extensively on Jupiter in the past (e.g. Fletcher et al., 2009; Nixon et al.,
225 2010). We assumed a globally homogeneous vertical atmospheric structure
226 using the temperature profile from Seiff et al. (1996). NH_3 , PH_3 , and CH_4
227 profiles were based on Fletcher et al. (2009), although these gases only con-
228 tribute minimally to the continuum in our spectral regions. H_2 and He
229 abundances were derived from Galileo probe measurements (Niemann et al.,
230 1998). We assumed equilibrium para- H_2 fraction throughout the atmosphere.
231 Aerosols have negligible opacity in the sub-mm and were not included in our
232 atmospheric model.

1
2
3
4
5
6
7
8
9
233 Collision induced absorption due to H₂-H₂, H₂-He, H₂-CH₄, and He-CH₄
10
234 pairs were included according to the formulations in Borysow et al. (1985,
11
12
235 1988); Borysow and Frommhold (1986, 1987); and Borysow (1991). Spectro-
13
14
236 scopic data were taken from HITRAN2004 (Rothman et al., 2005). NEME-
15
16
237 SIS uses the correlated-*k* approximation to calculate atmospheric opacity
17
18
238 (Goody and Yung, 1989; Lacis and Oinas, 1991), so we incorporated the
19
20
239 doppler lineshapes from section 3.2 directly into the *k*-tables for computa-
21
22
240 tional efficiency. The emission angle was assumed to be the Airy-weighted
23
24
241 disc-averaged emission angle from section 3.2.

26
242 We considered two end member HCl reference profiles: the first had con-
27
28
243 stant volume mixing ratio HCl for pressures lower than 1 mbar, and zero
29
30
244 HCl at higher pressures (subsequently referred to as [1 mbar]); and the sec-
31
32
245 ond was the profile given by the 1D diffusion model from Showman (2001)
33
34
246 (subsequently referred to as [S01]). Each reference profile had HCl set to
35
36
247 a uniform 1 ppb for all pressures less than 1 mbar. The [S01] 1D diffusion
37
38
248 profile is appropriate for an external source at or above the 1 mbar pressure
39
40
249 level with no HCl loss processes other than dilution with the bulk atmosphere
41
42
250 due to eddy mixing. Conversely, the [1 mbar] profile is appropriate if HCl
43
44
251 loss processes are significant in the middle stratosphere. Figure 4 shows the
45
46
252 assumed temperature profile, reference HCl profiles, contribution functions,
47
48
253 and corresponding synthetic spectra.

254 5. HCl upper limits

255 To calculate upper limits for HCl we follow a forward modelling approach
256 similar to Teanby et al. (2013) and Teanby and Irwin (2013). Reference pro-

1
2
3
4
5
6
7
8
9
10 257 files were scaled, then used to calculate synthetic spectra, which were com-
11 258 pared to the observations. For a given 1 mbar HCl abundance α we calculate
12
13 259 the misfit $\chi^2(\alpha)$ between the measured brightness temperature difference
14
15 260 spectra $y_i \pm \sigma_i$ and a synthetic brightness temperature difference spectrum
16
17 261 $f_i(\alpha)$:

$$\chi^2(\alpha) = \sum_{i=1}^n \frac{(y_i - f_i(\alpha))^2}{\sigma_i^2} \quad (2)$$

18
19
20
21
22
23 262 where both measured and synthetic spectra are defined at n frequencies ν_i
24
25 263 with $i = 1 \dots n$. The best fitting HCl abundance α_{opt} is where $\chi^2(\alpha)$ is
26
27 264 minimised. There is one free parameter (α), so for the abundance to be
28
29 265 significant at the $3\text{-}\sigma$ level $\Delta\chi^2 = \chi^2(\alpha_{\text{opt}}) - \chi^2(0)$ must be less than -9
30
31 266 (Press et al., 1992). In the case of no significant minimum, the $3\text{-}\sigma$ upper
32
33 267 limit is given by the value of α where $\Delta\chi^2 = +9$.

34
35 268 Figure 5 shows the variation of χ^2 as a function of 1 mbar HCl abundance
36
37 269 derived from scaling each of the two reference profiles, for band 1 and band 7.
38
39 270 No significant minima are present, indicating that we can only derive upper
40
41 271 limits from these data. Band 1 and band 7 data are consistent with each
42
43 272 other, but overall band 7 provides the most stringent constraint on Jupiter's
44
45 273 stratospheric HCl. The $3\text{-}\sigma$ upper limits on HCl abundance at 1 mbar are:
46
47 274 0.024 ppb when scaling the [S01] profile; and 0.056 ppb when using the
48
49 275 [1 mbar] profile. Figure 6 shows the measured spectra along with a $3\text{-}\sigma$
50
51 276 synthetics for comparison.

1
2
3
4
5
6
7
8
9 **277 6. Discussion**

10
11 *278 6.1. Possible external sources of chlorine*

12
13
14 *279* We can gain insight into potential sources of chlorine by combining our
15
16 *280* HCl upper limits with the derived oxygen flux into Jupiter, which has the
17
18 *281* advantage that oxygen species have actually been detected so are far better
19
20 *282* constrained. Bézard et al. (2002) and Lellouch et al. (2002) show that most
21
22 *283* of Jupiter’s stratospheric oxygen is in the form of CO, H₂O, or CO₂. These
23
24 *284* species have strong vertical gradients in the stratosphere consistent with an
25
26 *285* external source. Potential oxygen sources include interplanetary dust par-
27
28 *286* ticles, micrometeorites, comets, and Io’s plasma torus. Most of Jupiter’s
29
30 *287* stratospheric oxygen is in the form of CO. This is unusual, given that H₂O
31
32 *288* should be more abundant in interplanetary dust particles (IDPs), micromete-
33
34 *289* teorites, and comets and suggests that shock chemistry during large impacts
35
36 *290* is required to convert H₂O to CO (Bézard et al., 2002). IDPs and microm-
37
38 *291*eteorite impacts would not produce enough energy to convert H₂O to CO
39
40 *292* so 0.3–1.6 km sized comet impacts are preferred by Bézard et al. (2002).
41
42 *293* The CO production rate required to explain Bézard et al. (2002)’s observa-
43
44 *294* tions is 4×10^6 molecules/cm²/s and is the dominant production rate of any
45
46 *295* oxygen species in the upper atmosphere. Therefore, we can constrain the
47
48 *296* total oxygen influx (initially in either CO or H₂O molecular form) to also be
49
50 *297* 4×10^6 molecules/cm²/s. We now use this flux to predict chlorine flux for
51
52 *298* different source assumptions:

- 53
54 *299* • If the chlorine source is from comets, a solar Cl/O ratio of 6.9×10^{-4}
55
56 *300* is reasonable (Grevesse et al., 2007), implying a chlorine flux of $2.8 \times$
57
58 *301* 10^3 molecules/cm²/s. IDPs and micrometeorites can be discounted

1
2
3
4
5
6
7
8
9
302 as they would not result in sufficient CO production, but would also
10
11 provide a similar chlorine flux.
12

- 13
14 • If both the oxygen and the chlorine source is Io’s plasma torus, we can
15
16 use the observed Cl/O ration from Küppers and Schneider (2000) of
17
18 1/15 to derive a chlorine flux of 2.7×10^5 molecules/cm²/s - around 100
19
20 times that expected from comets. This flux would correspond to about
21
22 10% of Io’s plasma torus eventually entering Jupiter’s atmosphere. This
23
24 scenario seems unlikely given the shock chemistry arguments required
25
26 to explain the oxygen species, but is considered for completeness.
27

28 These predictions can now be compared to our HCl upper limits using a
29
30 numerical 1D diffusion model with and without loss processes.
31

32 33 6.2. Diffusion model HCl profile predictions with no loss 34

35 We start by assuming that all external chlorine forms HCl and the only
36
37 process operating is dilution with a HCl-free bulk troposphere via eddy mix-
38
39 ing. We then formulated a numerical 1D diffusion model by adapting the an-
40
41 alytical model outlined in Showman (2001). Briefly, we split the atmosphere
42
43 into N layers of equal thickness Δz with altitudes z_i where $i = 1 \dots N$ cover-
44
45 ing pressures from 10 bar to 1 mbar. The upward flux of HCl was determined
46
47 using:
48

$$49 \quad \phi(z) = -K(z) \left[\frac{dn(z)}{dz} + \frac{n(z)}{H(z)} + \frac{n(z)}{T(z)} \left(\frac{dT(z)}{dz} \right) \right] \quad (3)$$

50
51

52 where $K(z)$ is the eddy diffusion coefficient, $n(z)$ is the number density of
53
54 HCl, $H(z)$ is the atmospheric scale height (RT/Mg), and $T(z)$ is the tem-
55
56 perature (Showman, 2001; Chamberlain and Hunten, 1987). The bottom
57
58

1
2
3
4
5
6
7
8
9
324 boundary condition was defined by:

$$n(z_1) = \frac{\phi(z_1)H(z_1)}{K(z_1)} \quad (4)$$

325 The HCl profile was then calculated using a finite-difference time-stepping
326 approach in which the change in HCl number density at each level z_j in time
327 Δt was given by the approximation:

$$\Delta n(z_j) = \frac{(\phi(z_{j-1}) - \phi(z_{j+1}))}{2\Delta z} \Delta t \quad (5)$$

328 We set an input flux of $-\phi_0$ at the model top, where ϕ_0 is the (downward)
329 input flux from our source scenario. For the first time step, $n(z)$ is initialised
330 to zero at all levels except for the top level, which has $n(z_N) = -\phi_0\Delta t/\Delta z$.
331 The model was then iterated for 1000 model years with 1hr time steps to
332 determine the steady state HCl profile, which is independent of the initial HCl
333 profile. This numerical model reproduces the analytical solution presented in
334 Showman (2001) under equivalent assumptions, but provides the additional
335 flexibility needed to include loss processes.

336 Figure 7 shows the model parameters and predicted HCl profiles for input
337 HCl fluxes of 2.8×10^3 and 2.7×10^5 molecules/cm²/s. These profiles are
338 effectively scaled versions of each other; as we have not yet included any
339 loss processes, the HCl abundance at each level is simply a function of the
340 input flux and the eddy diffusion. The model predicts HCl abundances at
341 1 mbar of 0.05 ppb (for 2.8×10^3 molecules/cm²/s from comets) and 5 ppb
342 (for 2.7×10^5 molecules/cm²/s from Io). These can be considered maximum
343 values as loss has been neglected and also because not all externally supplied
344 Cl will be in form of HCl. Recent observations of comet Hartley 2 (Bockelée-
345 Morvan et al., 2014) suggest HCl is sub-solar in comets and chlorine could

1
2
3
4
5
6
7
8
9 346 hence be in other forms. However, it is reasonable to assume that reduction
10 347 in Jupiter's hydrogen-rich upper atmosphere would lead to creation of HCl,
11
12 348 at least initially.

13
14
15 349 If loss processes in the upper stratosphere can be ignored, our upper limits
16 350 are most consistent with the lower Cl flux predicted by an approximately solar
17
18 351 composition external source. If Io were the source, at least 200 times more
19
20 352 HCl would be expected than our observations suggest. However, even a solar
21
22 353 composition external source predicts too much HCl - 0.05 ppb compared to
23
24 354 our upper limit of 0.024 ppb. This suggests HCl loss processes are important
25
26 355 in Jupiter's upper stratosphere and cannot be ignored.

27 28 29 356 *6.3. Diffusion model HCl profile predictions with aerosol scavenging*

30
31
32 357 Our modelling suggests that stratospheric HCl loss processes must be
33
34 358 considered in order to explain the very low upper limits. Therefore, we now
35
36 359 consider the effect of potential loss mechanisms for HCl in the stratosphere.
37
38 360 Scavenging by stratospheric aerosols could be a significant sink of HCl. To
39
40 361 model this we first define an accommodation coefficient, γ , which is the frac-
41
42 362 tion of HCl-aerosol collisions that result in HCl sticking to the aerosol and
43
44 363 being scavenged. This parameter is poorly constrained and will depend on
45
46 364 the precise composition and physical structure of the aerosol, so we treat it
47
48 365 as a free parameter in the model. Values of γ in the range 0.1–1 seem rea-
49
50 366 sonable based terrestrial scavenging processes (Tabazadeh and Turco, 1993;
51
52 367 Davis, 2006), especially for droplets of water (Schweitzer et al., 2000), impure
53
54 368 water solutions (Li et al., 2002; Rudich, 2003) or ammonia (see discussion in
55
56 369 Showman, 2001). However, such droplets are unlikely to be representative
57
58 370 of Jupiter's upper stratosphere aerosols, which are most likely to be based

1
2
3
4
5
6
7
8
9
371 on photochemically produced hydrocarbons. Experiments on organic com-
10
372 pounds suggest γ could be much lower; perhaps as low as 0.001–0.01 (Zhang
11
12
13 373 et al., 2003) for experiments with octanol. It is possible that values of γ for
14
15 374 scavenging by Jupiter’s aerosols could be even lower. Therefore, to cover the
16
17 375 large uncertainty, we consider γ ’s in the range 10^{-5} –1.0 as well as $\gamma = 0$,
18
19 376 which represents no loss.

20
377 To determine the number of HCl-aerosol collisions, we also require the
21
22 378 aerosol properties, specifically their number density and radii as a function
23
24 379 of altitude. These are also poorly constrained in the upper stratosphere,
25
26 380 so we use the values from the model of Banfield et al. (1998) to estimate
27
28 381 the magnitude of the scavenging effect. This model includes aerosol growth
29
30 382 during descent through the atmosphere.

31
32 383 To determine collision rates, consider an ideal gas containing HCl molecules
33
34 384 and aerosol particles. From gas kinetic theory (e.g. Tabor, 1993; Woan, 2003),
35
36 385 the mean speed \bar{c} of the HCl molecules is given by:

$$\bar{c} = \left(\frac{8kT(z)}{\pi m} \right)^{1/2} \quad (6)$$

37
38 386 where k is the Boltzmann constant and m is the mass of one HCl molecule,
39
40 387 resulting in typical speeds of 310 ms^{-1} at 1 mbar in Jupiter’s upper strato-
41
42 388 sphere. The aerosol particles, being relatively heavy, can be assumed to be
43
44 389 effectively stationary with respect to the rapidly moving HCl molecules. The
45
46 390 aerosol particles have a relatively large radius r_a of order $0.1 \mu\text{m}$, so the HCl
47
48 391 molecules can be assumed to have negligible radius. This implies that a HCl-
49
50 392 aerosol collision will occur if a HCl molecule comes within r_a of an aerosol
51
52 393 particle. Therefore, in time t a single HCl molecule sweeps out a potential
53
54 394 collision volume $V = \pi r_a^2 \bar{c} t$. If the number density of aerosol particles is n_a ,
55
56
57
58
59
60
61
62
63
64
65

1
2
3
4
5
6
7
8
9
395 this results in $\pi r_a^2 \bar{c} n_a$ collisions per second, with an average time between
10 collisions of $\delta t = 1/\pi r_a^2 \bar{c} n_a$. The probability $P(x)$ of a HCl molecule not
11
12
13 397 colliding with an aerosol particle is given by the survival equation:

$$14 \quad P(x) = \exp(-x/\lambda) \quad (7)$$

15
16
17
18 398 where $x = \bar{c}\Delta t$ is the distance travelled in each time step and $\lambda = \bar{c}\delta t$ is the
19 mean free path (Tabor, 1993). If a fraction γ of collisions result in scavenging
20 399 of the HCl molecule by the aerosol particle, the probability $P'(t)$ of a HCl
21
22 400 molecule being scavenged in time t is:

$$23 \quad P'(t) = \gamma(1 - \exp(-t/\delta t)) \quad (8)$$

24
25
26
27
28
29 402 So after each time step Δt , the fraction of HCl remaining $R(\Delta t)$ is given by:

$$30 \quad R(\Delta t) = 1 - \gamma(1 - \exp(-\pi r_a^2 \bar{c} n_a \Delta t)) \quad (9)$$

31
32
33
34
35 403 This loss process was applied to the HCl number density $n(z)$ after each time
36
37 404 step in our diffusion model.

38
39 405 Figure 7 shows the resulting HCl profiles for HCl injection at 1 mbar and
40 a reasonable range of values for γ . Unless HCl-aerosol collisions are extremely
41 406 inefficient at scavenging, HCl is removed very quickly and cannot build up
42
43 407 in observable quantities. If we assume aerosol scavenging is the sole loss
44
45 408 process, our upper limits can be used to place moderate constraints on the
46
47 409 chlorine source. For an Io based chlorine source, γ must be greater than 0.1
48
49 410 to be consistent with our upper limits, whereas for solar composition source
50
51 411 γ need only be greater than 10^{-5} . Based on the literature, low values of γ
52
53 412 appear more likely for organic aerosols, which argues for a solar composition
54
55 413 source. However, there are many uncertainties in our model, for example,
56
57 414

1
2
3
4
5
6
7
8
9 415 if HCl injection is higher in the atmosphere then scavenging could be even
10
11 416 more efficient due to the greater combined surface area of smaller aerosol
12
13 417 particles at higher altitudes.

14
15 418 Additional complications arise because aerosol scavenging is not the only
16
17 419 possible loss process: reactions with ammonia is another potential mecha-
18
19 420 nism. Scavenging by tropospheric NH_3 was considered in detail by Showman
20
21 421 (2001) and is not considered further here. We consider this to be a minor
22
23 422 process as most NH_3 is removed by cold trap, and any small residual would be
24
25 423 destroyed by photolysis well below 1 mbar pressure level (Atreya et al., 1977;
26
27 424 Atreya and Donahue, 1979). The effectiveness of NH_3 destruction in the at-
28
29 425 mosphere by photolysis is very efficient, as evidenced by the rapid depletion
30
31 426 in NH_3 injected by the SL9 impact (Fast et al., 2002; Moses et al., 1995).
32
33 427 Perhaps more important than tropospherically sourced NH_3 is periodic NH_3
34
35 428 injection by cometary impacts, which can provide significant transient NH_3
36
37 429 abundances at these altitudes, reaching >1 ppm over local scales (Fast et al.,
38
39 430 2002). Cometary impacts that penetrate deeper into the atmosphere may
40
41 431 also excavate tropospheric NH_3 into the stratosphere via entrainment in im-
42
43 432 pact plumes (Fletcher et al., 2011). Such transient NH_3 sources could easily
44
45 433 remove ppb amounts of HCl by formation and subsequent precipitation of
46
47 434 NH_4Cl salts.

48
49 435 Our extremely low HCl upper limits are suggestive of, and consistent
50
51 436 with, the estimated high efficiency of scavenging processes in Jupiter's up-
52
53 437 per stratosphere; either by aerosols or transient NH_3 from comet impacts.
54
55 438 Unfortunately, in the presence of such scavenging, we cannot unambiguously
56
57 439 distinguish between potential HCl sources, as both Io's plasma torus and

1
2
3
4
5
6
7
8
9
10 440 cometary input fluxes could be removed efficiently enough to prevent a de-
11 441 tection with Herschel. However, our observations and modelling are most
12
13 442 consistent with a cometary source for the supply of external material into
14
15 443 Jupiter’s upper atmosphere.

16
17 444 Figure 8 schematically summarises the implications of our observations
18
19 445 and modelling, combined with those from previous studies, for Jupiter’s chlo-
20
21 446 rine cycle.

22 23 24 447 **7. Conclusion**

25
26
27 448 We used Herschel’s HIFI spectrometer to derive stringent new upper lim-
28
29 449 its for HCl in Jupiter’s atmosphere. For a profile that has constant HCl
30
31 450 above the 1 mbar level we obtain a 3- σ upper limit of 0.056 ppb, whereas
32
33 451 scaling a 1D diffusion model based profile with an upper atmosphere source
34
35 452 gives a 3- σ upper limit of 0.024 ppb. Therefore, if HCl is present in Jupiter’s
36
37 453 upper atmosphere it must be in extremely small amounts. For comparison,
38
39 454 the previous best upper limit was 2.3 ppb (Fouchet et al., 2004) at around
40
41 455 0.5 bar. Our lossless diffusion model combined with a source with solar Cl/O
42
43 456 relative abundances would predict abundances of ~ 0.05 ppb at the 1 mbar
44
45 457 pressure level and $\sim 1-2 \times 10^{-14}$ at the 0.5 bar pressure level.

46
47 458 If HCl scavenging by stratospheric aerosols or ammonia is negligible, our
48
49 459 upper limits rule out Io’s plasma torus as a source for chlorine and are more
50
51 460 consistent with a source with a lower, approximately solar, Cl/O ratio such as
52
53 461 comets. However, our HCl upper limit is lower than the abundance predicted
54
55 462 by such a source, which suggests that HCl scavenging of some kind is indeed
56
57 463 occurring. Therefore, based on this and on our modelling, negligible loss of

1
2
3
4
5
6
7
8
9 464 HCl in the upper stratosphere seems highly unlikely.

10
11 465 Our modelling suggests that scavenging by stratospheric aerosols is likely
12
13 466 to be a significant loss process, and is very efficient for reasonable aerosol
14
15 467 number densities and accommodation coefficients. In the steady state atmo-
16
17 468 sphere, scavenging of HCl by internally sourced NH_3 is unlikely as it would
18
19 469 be destroyed by photolysis at much lower altitudes. However, NH_3 transients
20
21 470 caused by cometary impacts such as SL9 could be a very efficient further loss
22
23 471 mechanism, either by direct NH_3 injection or by dredging up deep NH_3 by
24
25 472 entrainment of tropospheric material in impact plumes. The efficiency of po-
26
27 473 tential loss mechanisms limits our ability to constrain the source of Jupiter's
28
29 474 chlorine flux. However, our results favour a solar composition source (such
30
31 475 as comets) because less extreme aerosol accommodation coefficients are re-
32
33 476 quired.

34 477 Further constraints on Jupiter's chlorine cycle would require laboratory
35
36 478 measurements of HCl accommodation coefficients and better quantification
37
38 479 of upper stratospheric aerosols. Direct detection of HCl would require an
39
40 480 increase in sensitivity of many orders of magnitude and seems unrealisable
41
42 481 given current technology.

43 44 45 482 **8. Acknowledgements**

46
47
48 483 This work was funded by the UK Science and Technology Facilities Coun-
49
50 484 cil, the Leverhulme Trust, the NASA Planetary Atmospheres Program, and
51
52 485 the Royal Society. The authors would like to thank Mark Kidger, David
53
54 486 Teyssier, and Anthony Marston at the Herschel Science Centre for help with
55
56 487 observation planning and design. HIFI has been designed and built by a

1
2
3
4
5
6
7
8
9 488 consortium of institutes and university departments from across Europe,
10
11 489 Canada and the United States under the leadership of SRON Netherlands
12
13 490 Institute for Space Research, Groningen, The Netherlands and with major
14
15 491 contributions from Germany, France and the US. Consortium members are:
16
17 492 Canada: CSA, U.Waterloo; France: CESR, LAB, LERMA, IRAM; Germany:
18
19 493 KOSMA, MPIfR, MPS; Ireland, NUI Maynooth; Italy: ASI, IFSI-INAF, Os-
20
21 494 servatorio Astrofisico di Arcetri-INAF; Netherlands: SRON, TUD; Poland:
22
23 495 CAMK, CBK; Spain: Observatorio Astronmico Nacional (IGN), Centro de
24
25 496 Astrobiologa (CSIC-INTA). Sweden: Chalmers University of Technology -
26
27 497 MC2, RSS & GARD; Onsala Space Observatory; Swedish National Space
28
29 498 Board, Stockholm University - Stockholm Observatory; Switzerland: ETH
30
31 499 Zurich, FHNW; USA: Caltech, JPL, NHSC. HCSS / HSpot / HIPE is a
32
33 500 joint development (are joint developments) by the Herschel Science Ground
34
35 501 Segment Consortium, consisting of ESA, the NASA Herschel Science Center,
36
37 502 and the HIFI, PACS and SPIRE consortia.

39 503 **References**

- 40
41
42 504 Atreya, S.K., Donahue, T.M., 1979. Models of the Jovian Upper Atmosphere.
43
44 505 Rev. Geophys. & Space Phys. 17, 388–396.
- 45
46
47 506 Atreya, S.K., Donahue, T.M., Kuhn, W.R., 1977. The distribution of am-
48
49 507 monia and its photochemical products on Jupiter. Icarus 31, 348–355.
- 50
51
52 508 Banfield, D., Conrath, B.J., Gierasch, P.J., Nicholson, P.D., Matthews, K.,
53
54 509 1998. Near-IR Spectrophotometry of Jovian aerosols - meridional and
55
56 510 vertical distributions. Icarus 134, 11–23.

1
2
3
4
5
6
7
8
9
10
11
12
13
14
15
16
17
18
19
20
21
22
23
24
25
26
27
28
29
30
31
32
33
34
35
36
37
38
39
40
41
42
43
44
45
46
47
48
49
50
51
52
53
54
55
56
57
58
59
60
61
62
63
64
65

511 Bézard, B., Lellouch, E., Strobel, D., Maillard, J.P., Drossart, P., 2002.
512 Carbon Monoxide on Jupiter: Evidence for Both Internal and External
513 Sources. *Icarus* 159, 95–111.

514 Bockelée-Morvan, D., Biver, N., Crovisier, J., Lis, D.C., Hartogh, P., Moreno,
515 R., de Val-Borro, M., Blake, G.A., Szutowicz, S., Boissier, J., Cernicharo,
516 J., Charnley, S.B., Combi, M., Cordiner, M.A., de Graauw, T., Encrenaz,
517 P., Jarchow, C., Kidger, M., Küppers, M., Milam, S.N., Müller, H.S.P.,
518 Phillips, T.G., Rengel, M., 2014. Searches for HCl and HF in comets
519 103P/Hartley 2 and C/2009 P1 (Garradd) with the Herschel Space Obser-
520 vatory. *Astron. Astrophys.* 562, A5. 1401.1104.

521 Borysow, A., 1991. Modelling of collision-induced infrared-absorption spectra
522 of H₂-H₂ pairs in the fundamental band at temperatures from 20K to 300K.
523 *Icarus* 92, 273–279.

524 Borysow, A., Frommhold, L., 1986. Theoretical collision-induced rototrans-
525 lational absorption spectra for the outer planets: H₂-CH₄ pairs. *Astrophys.*
526 *J.* 304, 849–865.

527 Borysow, A., Frommhold, L., 1987. Collision-induced rototranslational ab-
528 sorption spectra of CH₄-CH₄ pairs at temperatures from 50 to 300K. *As-*
529 *trophys. J.* 318, 940–943.

530 Borysow, J., Frommhold, L., Birnbaum, G., 1988. Collision-induced roto-
531 translational absorption-spectra of H₂-He pairs at temperatures from 40
532 to 3000 k. *Astrophys. J.* 326, 509–515.

1
2
3
4
5
6
7
8
9
10
11
12
13
14
15
16
17
18
19
20
21
22
23
24
25
26
27
28
29
30
31
32
33
34
35
36
37
38
39
40
41
42
43
44
45
46
47
48
49
50
51
52
53
54
55
56
57
58
59
60
61
62
63
64
65

533 Borysow, J., Trafton, L., Frommhold, L., Birnbaum, G., 1985. Modeling
534 of pressure-induced far-infrared absorption-spectra: molecular-hydrogen
535 pairs. *Astrophys. J.* 296, 644–654.

536 Chamberlain, J.W., Hunten, D.M., 1987. Theory of planetary atmospheres.
537 An introduction to their physics and chemistry. Number 36 in International
538 Geophysics Series, Academic Press Inc., Orlando. 2nd edition.

539 Davis, E.J., 2006. A history and state-of-the-art of accommodation coeffi-
540 cients. *Atmospheric Research* 82, 561–578.

541 de Graauw, T., Helmich, F.P., Phillips, T.G., Stutzki, J., Caux, E., Why-
542 born, N.D., Dieleman, P., Roelfsema, P.R., Aarts, H., Assendorp, R.,
543 Bachiller, R., Baechtold, W., Barcia, A., Beintema, D.A., Belitsky, V.,
544 Benz, A.O., Bieber, R., Boogert, A., Borys, C., Bumble, B., Caïs, P., Caris,
545 M., Cerulli-Irelli, P., Chattopadhyay, G., Cherednichenko, S., Ciechanow-
546 icz, M., Coeur-Joly, O., Comito, C., Cros, A., de Jonge, A., de Lange,
547 G., Delforges, B., Delorme, Y., den Boggende, T., Desbat, J.M., Diez-
548 González, C., di Giorgio, A.M., Dubbeldam, L., Edwards, K., Eggens, M.,
549 Erickson, N., Evers, J., Fich, M., Finn, T., Franke, B., Gaier, T., Gal,
550 C., Gao, J.R., Gallego, J.D., Gauffre, S., Gill, J.J., Glenz, S., Golstein, H.,
551 Goulooze, H., Gunsing, T., Güsten, R., Hartogh, P., Hatch, W.A., Higgins,
552 R., Honingh, E.C., Huisman, R., Jackson, B.D., Jacobs, H., Jacobs, K.,
553 Jarchow, C., Javadi, H., Jellema, W., Justen, M., Karpov, A., Kasemann,
554 C., Kawamura, J., Keizer, G., Kester, D., Klapwijk, T.M., Klein, T., Koll-
555 berg, E., Kooi, J., Kooiman, P.P., Kopf, B., Krause, M., Krieg, J.M.,
556 Kramer, C., Kruiuzenga, B., Kuhn, T., Laauwen, W., Lai, R., Larsson, B.,

1
2
3
4
5
6
7
8
9
10
11
12
13
14
15
16
17
18
19
20
21
22
23
24
25
26
27
28
29
30
31
32
33
34
35
36
37
38
39
40
41
42
43
44
45
46
47
48
49
50
51
52
53
54
55
56
57
58
59
60
61
62
63
64
65

557 Leduc, H.G., Leinz, C., Lin, R.H., Liseau, R., Liu, G.S., Loose, A., López-
558 Fernandez, I., Lord, S., Lunge, W., Marston, A., Martín-Pintado, J.,
559 Maestrini, A., Maiwald, F.W., McCoey, C., Mehdi, I., Megej, A., Melchior,
560 M., Meinsma, L., Merkel, H., Michalska, M., Monstein, C., Moratschke, D.,
561 Morris, P., Muller, H., Murphy, J.A., Naber, A., Natale, E., Nowosielski,
562 W., Nuzzolo, F., Olberg, M., Olbrich, M., Orfei, R., Orleanski, P., Os-
563 senkopf, V., Peacock, T., Pearson, J.C., Peron, I., Phillip-May, S., Piazzo,
564 L., Planesas, P., Rataj, M., Ravera, L., Risacher, C., Salez, M., Samoska,
565 L.A., Saraceno, P., Schieder, R., Schlecht, E., Schlöder, F., Schmülling,
566 F., Schultz, M., Schuster, K., Siebertz, O., Smit, H., Szczerba, R., Ship-
567 man, R., Steinmetz, E., Stern, J.A., Stokroos, M., Teipen, R., Teyssier,
568 D., Tils, T., Trappe, N., van Baaren, C., van Leeuwen, B.J., van de Stadt,
569 H., Visser, H., Wildeman, K.J., Wafelbakker, C.K., Ward, J.S., Wesselius,
570 P., Wild, W., Wulff, S., Wunsch, H.J., Tielens, X., Zaal, P., Zirath, H.,
571 Zmuidzinas, J., Zwart, F., 2010. The Herschel-Heterodyne Instrument for
572 the Far-Infrared (HIFI). *Astron. Astrophys.* 518, L6.

573 Fast, K., Kostiuik, T., Romani, P., Espenak, F., Hewagama, T., Betz, A.,
574 Boreiko, R., Livengood, T., 2002. Temporal Behavior of Stratospheric
575 Ammonia Abundance and Temperature Following the SL9 Impacts. *Icarus*
576 156, 485–497.

577 Fegley, B., Lodders, K., 1994. Chemical models of the deep atmospheres of
578 Jupiter and Saturn. *Icarus* 110, 117–154.

579 Feuchtgruber, H., Lellouch, E., Encrenaz, T., Bezaud, B., Coustenis, A.,
580 Drossart, P., Salama, A., de Graauw, T., Davis, G.R., 1999. Oxygen in

1
2
3
4
5
6
7
8
9
10
11
12
13
14
15
16
17
18
19
20
21
22
23
24
25
26
27
28
29
30
31
32
33
34
35
36
37
38
39
40
41
42
43
44
45
46
47
48
49
50
51
52
53
54
55
56
57
58
59
60
61
62
63
64
65

581 the stratospheres of the giant planets and Titan, in: Cox, P., Kessler, M.
582 (Eds.), *The Universe as Seen by ISO*, pp. 133–136.

583 Feuchtgruber, H., Lellouch, E., de Graauw, T., Bézard, B., Encrenaz, T.,
584 Griffin, M., 1997. External supply of oxygen to the atmospheres of the
585 giant planets. *Nature* 389, 159–162.

586 Flasar, F.M., Kunde, V.G., Abbas, M.M., Achterberg, R.K., Ade, P.,
587 Barucci, A., Bézard, B., Bjoraker, G.L., Brasunas, J.C., Calcutt, S.,
588 Carlson, R., Esarsky, C.J.C., Conrath, B.J., Coradini, A., Courtin, R.,
589 Coustenis, A., Edberg, S., Edgington, S., Ferrari, C., Fouchet, T., Gau-
590 tier, D., Gierasch, P.J., Grossman, K., Irwin, P., Jennings, D.E., Lel-
591 louch, E., Mamoutkine, A.A., Marten, A., Meyer, J.P., Nixon, C.A., Or-
592 ton, G.S., Owen, T.C., Pearl, J.C., Prange, R., Raulin, F., Read, P.L.,
593 Romani, P.N., Samuelson, R.E., Segura, M.E., Showalter, M.R., Simon-
594 Miller, A.A., Smith, M.D., Spencer, J.R., Spilker, L.J., Taylor, F.W., 2004.
595 Exploring the Saturn system in the thermal infrared: The Composite In-
596 frared Spectrometer. *Space Sci. Rev.* 115, 169–297.

597 Fletcher, L.N., Orton, G.S., de Pater, I., Edwards, M.L., Yanamandra-Fisher,
598 P.A., Hammel, H.B., Lisse, C.M., Fisher, B.M., 2011. The aftermath of
599 the July 2009 impact on Jupiter: Ammonia, temperatures and particulates
600 from Gemini thermal infrared spectroscopy. *Icarus* 211, 568–586.

601 Fletcher, L.N., Orton, G.S., Teanby, N.A., Irwin, P.G.J., 2009. Phosphine
602 on Jupiter and Saturn from Cassini/CIRS. *Icarus* 202, 543–564.

603 Fletcher, L.N., Swinyard, B., Salji, C., Polehampton, E., Fulton, T., Sidher,

- 1
2
3
4
5
6
7
8
9
604 S., Lellouch, E., Moreno, R., Orton, G., Cavalié, T., Courtin, R., Ren-
10 gel, M., Sagawa, H., Davis, G.R., Hartogh, P., Naylor, D., Walker, H.,
11
12 605 Lim, T., 2012. Sub-millimetre spectroscopy of Saturn's trace gases from
13
14 606 Herschel/SPIRE. *Astron. Astrophys.* 539, A44.
15
16
17
18 608 Fouchet, T., Orton, G., Irwin, P.G.J., Calcutt, S.B., Nixon, C.A., 2004. Up-
19
20 609 per limits on hydrogen halides in Jupiter from Cassini/CIRS observations.
21
22 610 *Icarus* 170, 237–241.
23
24 611 Goody, R.M., Yung, Y.L., 1989. *Atmospheric Radiation: Theoretical Basis*.
25
26 612 Oxford University Press, Oxford. 2nd edition.
27
28
29 613 Grevesse, N., Asplund, M., Sauval, A.J., 2007. *The Solar Chemical Compo-*
30
31 614 *sition. Space Sci. Rev.* 130, 105–114.
32
33
34 615 Gubbins, D., 2004. *Time series analysis and inverse theory for geophysicists*.
35
36 616 Cambridge Univ. Press, Cambridge UK.
37
38
39 617 HIFI Observers' Manual, 2011. *HERSCHEL-HSC-DOC-0784*. Version 2.4,
40
41 618 http://herschel.esac.esa.int/Docs/HIFI/pdf/hifi_om.pdf.
42
43
44 619 Irwin, P., Teanby, N., de Kok, R., Fletcher, L., Howett, C., Tsang, C., Wil-
45
46 620 son, C., Calcutt, S., Nixon, C., Parrish, P., 2008. The NEMESIS planetary
47
48 621 atmosphere radiative transfer and retrieval tool. *J. Quant. Spectro. Rad.*
49
50 622 *Trans.* 109, 1136–1150.
51
52
53 623 Kerola, D.X., Larson, H.P., Tomasko, M.G., 1997. Analysis of the near-IR
54
55 624 spectrum of Saturn: a comprehensive radiative transfer model of its middle
56
57 625 and upper troposphere. *Icarus* 127, 190–212.
58
59
60
61
62
63
64
65

- 1
2
3
4
5
6
7
8
9
626 Küppers, M., Schneider, N.M., 2000. Discovery of chlorine in the Io torus.
10
627 Geophys. Res. Lett. 27, 513–516.
11
12
13
628 Lacis, A.A., Oinas, V., 1991. A description of the correlated k distribution
14
629 method for modeling nongray gaseous absorption, thermal emission, and
15
630 multiple-scattering in vertically inhomogeneous atmospheres. J. Geophys.
16
631 Res. 96, 9027–9063.
17
18
19
20
21
632 Lellouch, E., Bézard, B., Moses, J.I., Davis, G.R., Drossart, P., Feuchtgruber,
22
633 H., Bergin, E.A., Moreno, R., Encrenaz, T., 2002. The Origin of Water
23
634 Vapor and Carbon Dioxide in Jupiter’s Stratosphere. Icarus 159, 112–131.
24
25
26
27
28
635 Li, Y.Q., Zhang, H.Z., Davidovits, P., Jayne, J.T., Kolb, C.E., Worsnop,
29
636 D.R., 2002. Uptake of HCl(g) and HBr(g) on Ethylene Glycol Surfaces as
30
637 a Function of Relative Humidity and Temperature. J. Phys. Chem. A 106,
31
638 1220–1227.
32
33
34
35
36
639 Moses, J.I., Allen, M., Gladstone, G.R., 1995. Nitrogen and oxygen photo-
37
640 chemistry following SL9. Geophys. Res. Lett. 22, 1601–1604.
38
39
40
41
641 Niemann, H., Atreya, S., Carignan, G., Donahue, T., Haberman, J., Harpold,
42
642 D., Hartle, R., Hunten, D., Kasprzak, W., Mahaffy, P., Owen, T., Way,
43
643 S., 1998. The composition of the Jovian atmosphere as determined by the
44
644 Galileo probe mass spectrometer. J. Geophys. Res. 103, 22831–22846.
45
46
47
48
49
645 Nixon, C.A., Achterberg, R.K., Romani, P.N., Allen, M., Zhang, X., Teanby,
50
646 N.A., Irwin, P.G.J., Flasar, F.M., 2010. Abundances of Jupiter’s trace
51
647 hydrocarbons from Voyager and Cassini. Plan. & Space Sci. 58, 1667–
52
648 1680.
53
54
55
56
57
58

- 1
2
3
4
5
6
7
8
9
649 Noll, K.S., 1996. Halogens in the giant planets: upper limits to HBr in Saturn
10 and Jupiter. *Icarus* 124, 608–615.
11
12
13
651 Ott, S., 2010. The Herschel Data Processing System - HIPE and Pipelines -
14 Up and Running Since the Start of the Mission, in: Mizumoto, Y., Morita,
15 K.I., Ohishi, M. (Eds.), *Astronomical Data Analysis Software and Systems*
16 XIX, pp. 139–142.
17
18
19
20
21
22
655 Press, W.H., Flannery, B.P., Teukolsky, S.A., Vetterling, W.T., 1992. Nu-
23 merical Recipes. Cambridge Univ. Press, Cambridge UK. 2nd edition.
24
25
26
657 Roelfsema, P.R., Helmich, F.P., Teyssier, D., Ossenkopf, V., Morris, P.,
28 Olberg, M., Shipman, R., Risacher, C., Akyilmaz, M., Assendorp, R.,
29 Avruch, I.M., Beintema, D., Biver, N., Boogert, A., Borys, C., Braine,
30 J., Caris, M., Caux, E., Cernicharo, J., Coeur-Joly, O., Comito, C., de
31 Lange, G., Delforge, B., Dieleman, P., Dubbeldam, L., de Graauw, T.,
32 Edwards, K., Fich, M., Fiederus, F., Gal, C., di Giorgio, A., Herpin, F.,
33 Higgins, D.R., Hoac, A., Huisman, R., Jarchow, C., Jellema, W., de Jonge,
34 A., Kester, D., Klein, T., Kooi, J., Kramer, C., Laauwen, W., Larsson,
35 B., Leinz, C., Lord, S., Lorenzani, A., Luinge, W., Marston, A., Martín-
36 Pintado, J., McCoey, C., Melchior, M., Michalska, M., Moreno, R., Müller,
37 H., Nowosielski, W., Okada, Y., Orleński, P., Phillips, T.G., Pearson, J.,
38 Rabois, D., Ravera, L., Rector, J., Rengel, M., Sagawa, H., Salomons, W.,
39 Sánchez-Suárez, E., Schieder, R., Schlöder, F., Schmölling, F., Soldati,
40 M., Stutzki, J., Thomas, B., Tielens, A.G.G.M., Vastel, C., Wildeman,
41 K., Xie, Q., Xilouris, M., Wafelbakker, C., Whyborn, N., Zaal, P., Bell,
42 T., Bjerkele, P., De Beck, E., Cavalié, T., Crockett, N.R., Hily-Blant, P.,
43
44
45
46
47
48
49
50
51
52
53
54
55
56
57
58
59
60
61
62
63
64
65

- 1
2
3
4
5
6
7
8
9
673 Kama, M., Kaminski, T., Lefl6ch, B., Lombaert, R., de Luca, M., Makai,
10
11 674 Z., Marseille, M., Nagy, Z., Pacheco, S., van der Wiel, M.H.D., Wang, S.,
12
13 675 Yildiz, U., 2012. In-orbit performance of Herschel-HIFI. *Astron. Astro-*
14
15 676 *phys.* 537, A17.
- 16
17
18 677 Rothman, L.S., Jacquemart, D., Barbe, A., Benner, D.C., Birk, M., Brown,
19
20 678 L.R., Carleer, M.R., Chackerian, C., Chance, K., Coudert, L.H., Dana, V.,
21
22 679 Devi, V.M., Flaud, J.M., Gamache, R.R., Goldman, A., Hartmann, J.M.,
23
24 680 Jucks, K.W., Maki, A.G., Mandin, J.Y., Massie, S.T., Orphal, J., Perrin,
25
26 681 A., Rinsland, C.P., Smith, M.A.H., Tennyson, J., Tolchenov, R.N., Toth,
27
28 682 R.A., Vander Auwera, J., Varanasi, P., Wagner, G., 2005. The HITRAN
29
30 683 2004 molecular spectroscopic database. *J. Quant. Spectro. Rad. Trans.* 96,
31
32 684 139–204.
- 33
34 685 Rudich, Y., 2003. Laboratory perspectives on the chemical transformations
35
36 686 of organic matter in atmospheric particles. *Chem. Rev.* 103, 5097–5124.
- 37
38
39 687 Schweitzer, F., Mirabel, P., George, C., 2000. Uptake of Hydrogen Halides
40
41 688 by Water Droplets. *J. Phys. Chem. A* 104, 72–76.
- 42
43
44 689 Seiff, A., Kirk, D.B., Knight, T.C.D., Mihalov, J.D., Blanchard, R.C., Young,
45
46 690 R.E., Schubert, G., von Zahn, U., Lehmacher, G., Milos, F.S., Wang, J.,
47
48 691 1996. Structure of the Atmosphere of Jupiter: Galileo Probe Measure-
49
50 692 ments. *Science* 272, 844–845.
- 51
52 693 Showman, A.P., 2001. Hydrogen halides on Jupiter and Saturn. *Icarus* 152,
53
54 694 140–150.
- 55
56
57
58
59
60
61
62
63
64
65

- 1
2
3
4
5
6
7
8
9 695 Tabazadeh, A., Turco, R.P., 1993. Stratospheric chlorine injection by volcanic
10 eruptions - HCl scavenging and implications for ozone. *Science* 260, 1082–
11 1086.
12
13 697
14
15 698 Tabor, D., 1993. *Gases, liquids and solids: and other states of matter.*
16 Cambridge University Press, Cambridge. 3rd edition.
17
18 699
19
20 700 Teanby, N.A., Fletcher, L.N., Irwin, P.G.J., Fouchet, T., Orton, G.S., 2006.
21 New upper limits for hydrogen halides on Saturn derived from Cassini-
22 CIRS data. *Icarus* 185, 466–475.
23
24 702
25
26 703 Teanby, N.A., Irwin, P.G.J., 2013. An External Origin for Carbon Monoxide
27 on Uranus from Herschel/SPIRE? *Astrophys. J.* 775, L49.
28
29 704
30
31 705 Teanby, N.A., Irwin, P.G.J., Nixon, C.A., Courtin, R., Swinyard, B.M.,
32 Moreno, R., Lellouch, E., Rengel, M., Hartogh, P., 2013. Constraints
33 on Titan’s middle atmosphere ammonia abundance from Herschel/SPIRE
34 sub-millimetre spectra. *Plan. & Space Sci.* 75, 136–147.
35
36 707
37
38 708
39
40 709 Weisstein, E.W., Serabyn, E., 1996. Submillimeter line search in Jupiter and
41 Saturn. *Icarus* 123, 23–36.
42
43 710
44
45 711 Wilson, T.L., Rohlfs, K., Hüttemeister, S., 2009. *Tools of Radio Astronomy.*
46 Springer-Verlag, Berlin. 5th edition.
47
48 712
49
50 713 Woan, G., 2003. *The Cambridge Handbook of Physics Formulas.* Cambridge
51 University Press, Cambridge.
52
53 714
54
55 715 Wong, M.H., Mahaffy, P.R., Atreya, S.K., Niemann, H.B., Owen, T.C., 2004.
56
57
58
59
60
61
62
63
64
65

1
2
3
4
5
6
7
8
9
10
11
12
13
14
15
16
17
18
19
20
21
22
23
24
25
26
27
28
29
30
31
32
33
34
35
36
37
38
39
40
41
42
43
44
45
46
47
48
49
50
51
52
53
54
55
56
57
58
59
60
61
62
63
64
65

716 Updated Galileo probe mass spectrometer measurements of carbon, oxy-
717 gen, nitrogen, and sulfur on Jupiter. *Icarus* 171, 153–170.

718 Zhang, H.Z., Li, Y.Q., Davidovits, P., Williams, L.R., Jayne, J.T., Kolb,
719 C.E., Worsnop, D.R., 2003. Uptake of Gas-Phase Species by 1-Octanol.
720 2. Uptake of Hydrogen Halides and Acetic Acid as a Function of Relative
721 Humidity and Temperature. *J. Phys. Chem. A* 107, 6398–6407.

1
2
3
4
5
6
7
8
9
10
11
12
13
14
15
16
17
18
19
20
21
22
23
24
25
26
27
28
29
30
31
32
33
34
35
36
37
38
39
40
41
42
43
44
45
46
47
48
49
50
51
52
53
54
55
56
57
58
59
60
61
62
63
64
65

Observation	Band	ID	Date	Start (UT)	Dur. (s)	WBS Freq. Range (GHz)	Δf (MHz)	θ_H ($^{\circ}$ N)	Diam ($''$)	Range (AU)	e ($^{\circ}$)	DFWHM (MHz)
1342266402	1	B1A	07/03/2013	19:10:22	4640	624.2270 - 628.3560	0.5	3.05	38.29	5.149	39.86	35.39
1342266403	1	B1B	07/03/2013	20:00:22	4520	624.1505 - 628.2795	0.5	3.05	38.29	5.149	39.86	35.39
1342266404	1	B1C	07/03/2013	20:50:22	4440	624.3375 - 628.4665	0.5	3.05	38.28	5.150	39.86	35.39
1342266597	7	B7B	28/02/2013	02:10:42	2914	1875.5715 - 1878.1340	0.5	3.07	39.25	5.023	15.52	39.65
1342266598	7	B7b	28/02/2013	03:30:00	2914	1875.4975 - 1878.0600	0.5	3.07	39.24	5.024	15.52	39.65
1342266599	7	B7C	28/02/2013	04:47:18	2914	1875.6795 - 1878.2420	0.5	3.07	39.24	5.025	15.52	39.65

Table 1: Observation summary. The total integration time in each of the two HCl bands was split into three observation blocks. For each observation, both horizontal and vertical polarisations were measured. Parameters are: Dur., observation block duration; Δf , WBS frequency spacing; θ_H , sub-Herschel latitude; Diam, angular diameter of Jupiter; Range, Herschel-Jupiter distance; e , weighted mean emission angle; and DFWM, equivalent doppler FWHM of spectral lines.

1
2
3
4
5
6
7
8
9
10
11
12
13
14
15
16
17
18
19
20
21
22
23
24
25
26
27
28
29
30
31
32
33
34
35
36
37
38
39
40
41
42
43
44
45
46
47
48
49
50
51
52
53
54
55
56
57
58
59
60
61
62
63
64
65

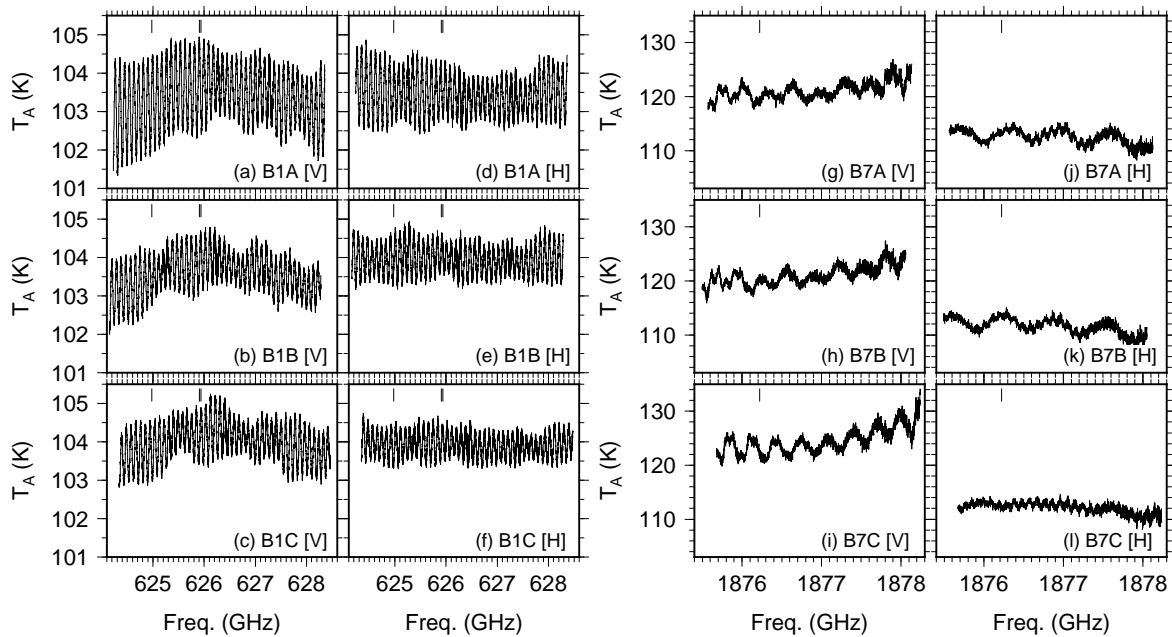


Figure 1: Antenna temperature spectra. Level 2 reduced Herschel/HIFI pipeline spectra for band 1 (a–f) and band 7 (g–l). [H] and [V] indicate horizontal and vertical polarisations respectively. All spectra suffer from standing wave interference: predominantly with periods of ~ 100 MHz in band 1 and ~ 320 MHz in band 7.

1
2
3
4
5
6
7
8
9
10
11
12
13
14
15
16
17
18
19
20
21
22
23
24
25
26
27
28
29
30
31
32
33
34
35
36
37
38
39
40
41
42
43
44
45
46
47
48
49
50
51
52
53
54
55
56
57
58
59
60
61
62
63
64
65

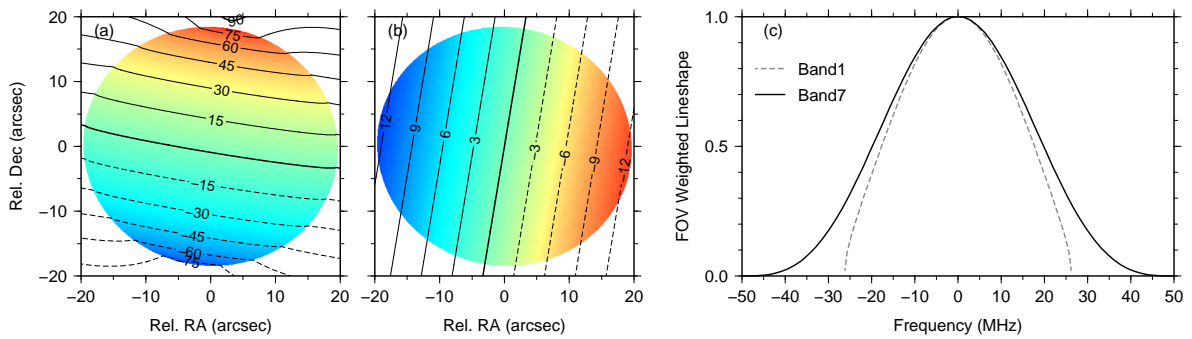


Figure 2: Effective doppler broadened lineshapes. (a) Orientation of Jupiter as viewed from Herschel during the HIFI observations. Contours show planetocentric latitude. (b) Line-of-sight velocity in km s^{-1} , where positive values are towards Herschel (blue-shifted). (c) Doppler broadened lineshapes, incorporating weighting by Herschel's Airy disc for band 1 (626.25 GHz) and band 7 (1876.75 GHz).

1
2
3
4
5
6
7
8
9
10
11
12
13
14
15
16
17
18
19
20
21
22
23
24
25
26
27
28
29
30
31
32
33
34
35
36
37
38
39
40
41
42
43
44
45
46
47
48
49
50
51
52
53
54
55
56
57
58
59
60
61
62
63
64
65

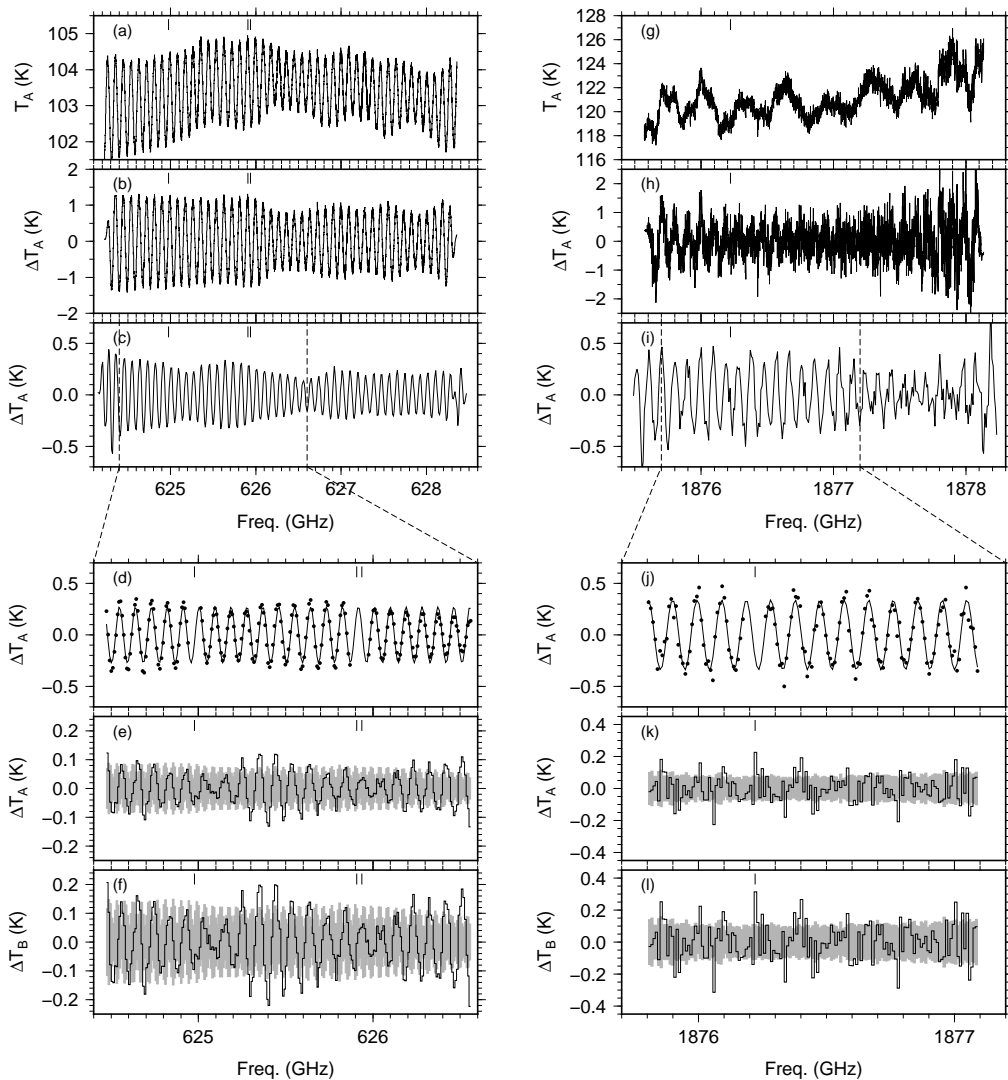


Figure 3: Data processing to reduce standing wave interference. (a) A single band 1 observation (vertical polarisation). (b) A single band 1 observation after application of a 200 MHz 4 pole high-pass Butterworth filter. (c) All six filtered horizontal and vertical polarisation observations for band 1 averaged with 9 MHz width bins to reduce random noise. (d) Zoom of a 2.2 GHz spectral segment, with the HCl line positions masked out, and a single frequency sine wave fitted to represent the standing wave contribution. (e) Residual spectrum after removal of the fitted sine wave. (f) Antenna temperature converted to brightness temperature. (g-l) The same procedure illustrated for band 7, which is identical to the process for band 1 except that the sine wave is fitted to a 1.5 GHz segment in this case. Vertical dashes near the top of each plot show the positions of HCl spectral lines. Grey envelopes indicate $1-\sigma$ errorbars.

1
2
3
4
5
6
7
8
9
10
11
12
13
14
15
16
17
18
19
20
21
22
23
24
25
26
27
28
29
30
31
32
33
34
35
36
37
38
39
40
41
42
43
44
45
46
47
48
49
50
51
52
53
54
55
56
57
58
59
60
61
62
63
64
65

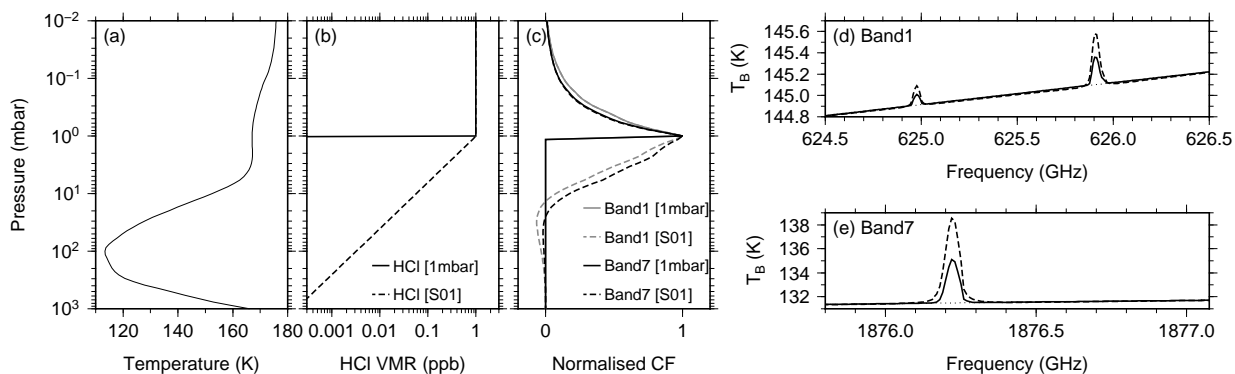


Figure 4: Predicted spectra for 1 ppb HCl at 1 mbar. (a) Assumed Jupiter pressure-temperature profile. (b) The two reference HCl profiles: [1 mbar] HCl uniformly mixed above 1 mbar and zero for higher pressures (solid lines); [S01] as [1 mbar] but with HCl abundances for higher pressures from the 1D diffusion model in Showman (2001) (dashed lines). (c) contribution functions at the HCl line centre for each of the reference profiles. Peak sensitivity of these observations is around 1 mbar with these profiles. (d,e) Synthetic spectra for band 1 and band 7 using the reference profiles and incorporating the doppler-broadened lineshape.

1
2
3
4
5
6
7
8
9
10
11
12
13
14
15
16
17
18
19
20
21
22
23
24
25
26
27
28
29
30
31
32
33
34
35
36
37
38
39
40
41
42
43
44
45
46
47
48
49
50
51
52
53
54
55
56
57
58
59
60
61
62
63
64
65

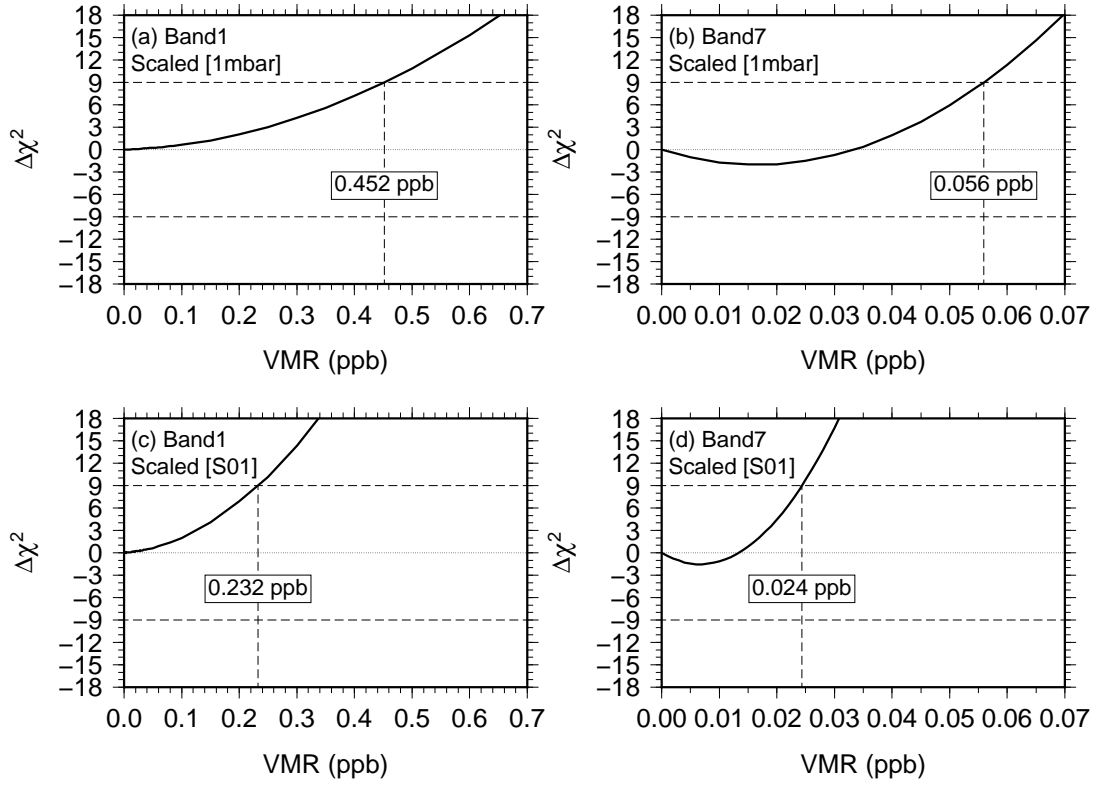


Figure 5: Variation of $\Delta\chi^2$ misfit as a function of HCl volume mixing ratio (VMR) at 1 mbar. (a,b) Band 1/band 7 with a scaled [1 mbar] reference profile. (c,d) Band 1/band 7 with a scaled [S01] reference profile. Dashed line at $\Delta\chi^2=-9$ shows the requirement for a 3- σ detection, which is not satisfied for either band 1 or band 7 spectra, indicating that HCl is not detected. Upper dashed line at $\Delta\chi^2=+9$ shows requirement for a 3- σ upper limit. VMRs in boxes give the upper limits for each profile and spectral band. Band 7 provides the most stringent constraints on HCl abundance.

1
2
3
4
5
6
7
8
9
10
11
12
13
14
15
16
17
18
19
20
21
22
23
24
25
26
27
28
29
30
31
32
33
34
35
36
37
38
39
40
41
42
43
44
45
46
47
48
49
50
51
52
53
54
55
56
57
58
59
60
61
62
63
64
65

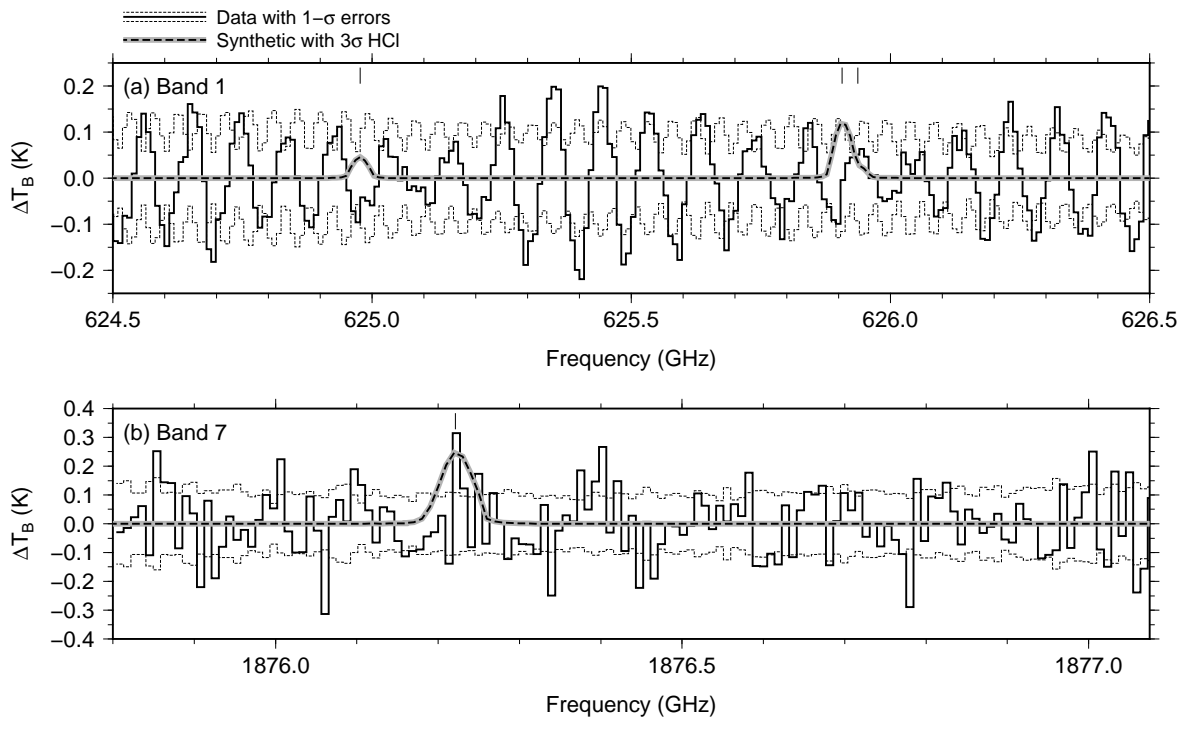


Figure 6: Synthetic spectra with upper limit abundances compared to observations. (a) Band 1 observation compared to a synthetic with 0.452 ppb HCl at 1 mbar using the [1 mbar] profile. (b) Band 7 observation compared to a synthetic with 0.056 ppb HCl at 1 mbar using the [1 mbar] profile. No significant HCl spectral features are visible in either set of observations. For band 7, there is a single bin displaying a high brightness temperature in the position of a HCl spectral line. However, the lineshape is incorrect, its height is comparable to other noise features, and the χ^2 analysis shows this not to be significant. Therefore, we regard this feature as spurious and attribute it to noise.

1
2
3
4
5
6
7
8
9
10
11
12
13
14
15
16
17
18
19
20
21
22
23
24
25
26
27
28
29
30
31
32
33
34
35
36
37
38
39
40
41
42
43
44
45
46
47
48
49
50
51
52
53
54
55
56
57
58
59
60
61
62
63
64
65

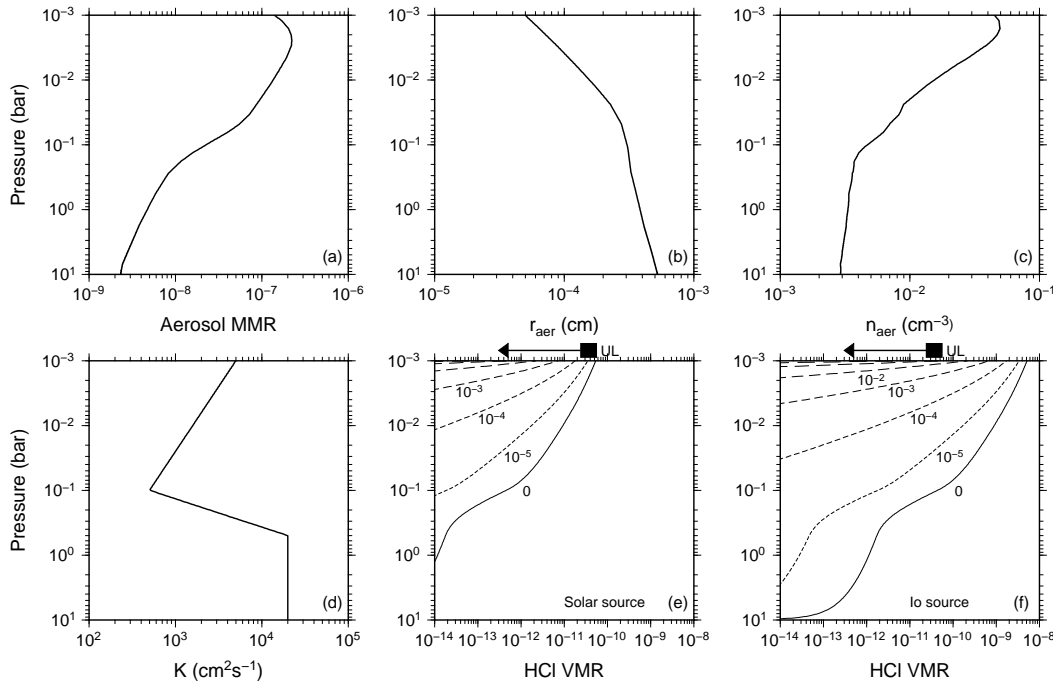


Figure 7: Diffusion model of HCl mixing and scavenging. (a) Aerosol mass mixing ratio (grammes of aerosol per gramme of atmosphere) from Banfield et al. (1998). (b) Aerosol radii profile from Banfield et al. (1998). (c) Number density of aerosols in the model. (d) Eddy diffusion profile used in the model (taken from Showman (2001)). (e) Predicted HCl profile for an external Cl flux of 2.8×10^3 molecules/ cm^2/s injected at 1 mbar, appropriate for a solar composition source (such as comets). Labelled lines indicate predicted HCl profiles for HCl-aerosol scavenging accommodation coefficients of $\gamma=0, 10^{-5}, 10^{-4}, 10^{-3}, 10^{-2}, 0.1,$ and 1. Black box with arrow at 1 mbar indicates upper limits derived from our Herschel/HIFI observations. Any value of γ over 10^{-4} – 10^{-5} gives a result consistent with our observations. (f) as for (e) except for an external Cl flux of 2.7×10^5 molecules/ cm^2/s , appropriate for a Cl and O source from Io. A value of γ of at least 0.1 is required to be consistent with our observations, which is most probably too high given current lab measurements with organic compounds.

1
2
3
4
5
6
7
8
9
10
11
12
13
14
15
16
17
18
19
20
21
22
23
24
25
26
27
28
29
30
31
32
33
34
35
36
37
38
39
40
41
42
43
44
45
46
47
48
49
50
51
52
53
54
55
56
57
58
59
60
61
62
63
64
65

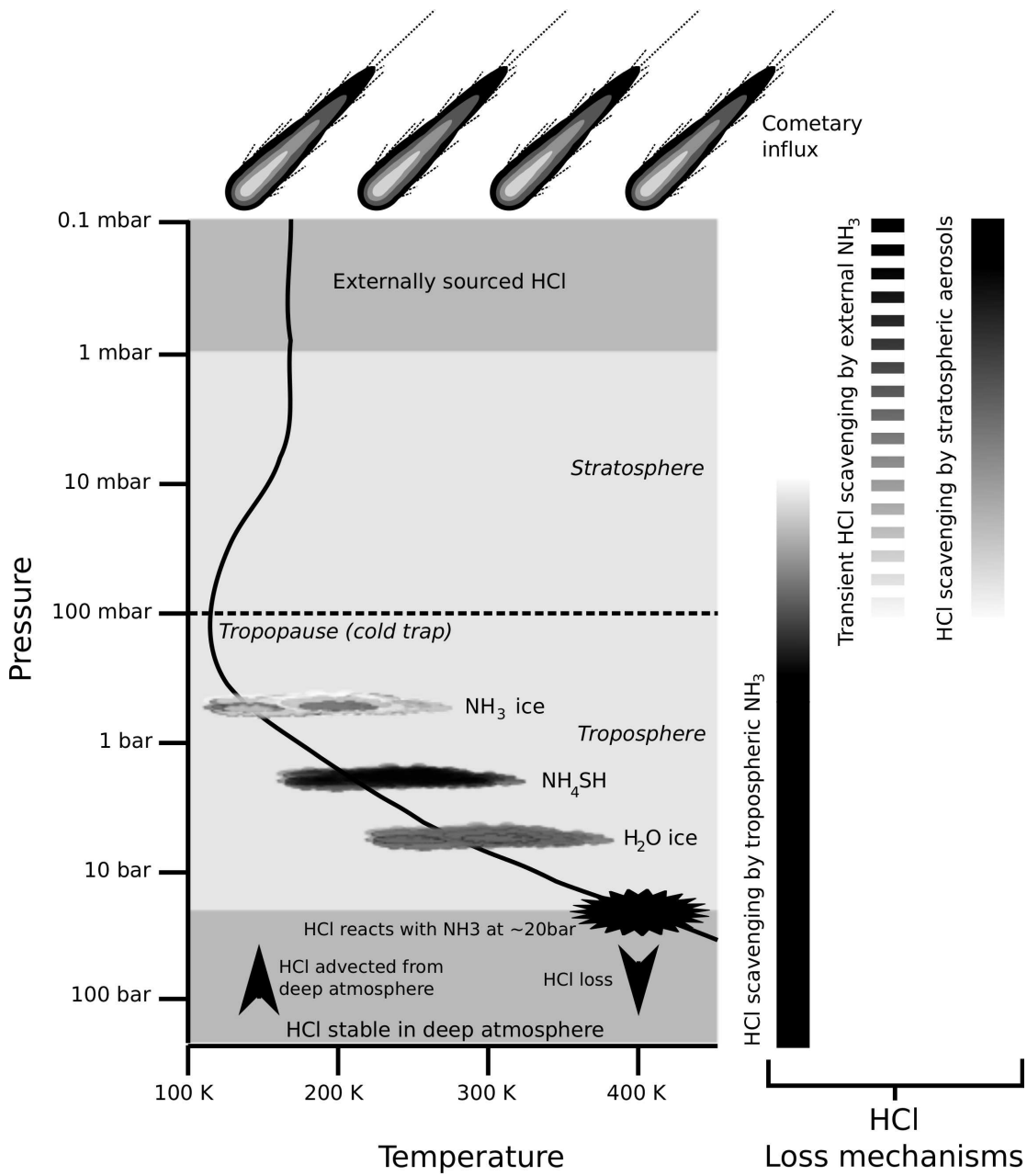


Figure 8: Schematic of Jupiter's chlorine cycle. Deep HCl lofted by convection becomes unstable at temperatures of 400K or less and reacts with NH₃ to form NH₄Cl and is recycled back into the deep atmosphere. Any residual HCl from the deep interior is scavenged by tropospheric NH₃ up until pressure levels of around 10 mbar, where all NH₃ will have been effectively removed by the tropopause cold trap and photolysis. Above the 1 mbar pressure level, externally sourced Cl forms HCl, but is most likely scavenged by stratospheric aerosols (a continuous/global process indicated with solid vertical bar) and externally sourced or impact plume excavated NH₃ (a transient/local process indicated by broken vertical bar).